Polymer 264 (2023) 125514

Contents lists available at ScienceDirect

Polymer

journal homepage: www.elsevier.com/locate/polymer

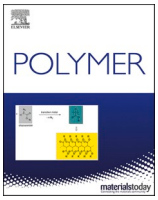

Understanding polymer nucleation by studying droplets crystallization in immiscible polymer blends

Seif Eddine Fenni [a,b], Alejandro J. Müller [c,d,*], Dario Cavallo [e,**]

[a] Mines Paris, PSL Research University, Centre de Mise en Forme des Matériaux (CEMEF), UMR CNRS 7635, CS 10207, 06904, Sophia Antipolis, France
[b] Institut Clément Ader (ICA), Université de Toulouse, CNRS, IMT Mines Albi, UPS, INSA, ISAE-SUPAERO, Campus Jarlard, F-81013, Albi, France
[c] Polymat and Department of Polymers and Advanced Materials: Physics, Chemistry and Technology, Faculty of Chemistry, University of the Basque Country UPV/EHU, Paseo Manuel de Lardizabal 3, 20018, Donostia-San Sebastián, Spain
[d] IKERBASQUE, Basque Foundation for Science, Plaza Euskadi 5, 48009, Bilbao, Spain
[e] Department of Chemistry and Industrial Chemistry, University of Genoa, Via Dodecaneso 31, 16146, Genova, Italy

ARTICLE INFO

Keywords:
Droplets dispersion
Surface nucleation
Turnbull number
Overall crystallization
Nucleating agents

ABSTRACT

This Feature Article reviews our recent work on the nucleation and crystallization of finely dispersed semi-crystalline polymeric droplets in immiscible matrices. Droplets dispersions can be used as a toolbox to investigate polymer nucleation. Studying the overall crystallization kinetics of the droplets can be a way to separate the contributions of nucleation and growth rates depending on the sample. To characterize the relative importance of nucleation versus growth, we have defined a dimensionless parameter named the "Turnbull number". This number equals the ratio of the time needed for a crystal to grow inside the average droplet volume, divided by the required time for nucleation to occur in the same droplet. We show examples for Turnbull numbers close to unity, where the overall crystallization kinetics of the droplets is dominated by crystal growth, and a sigmoidal (second or third order) kinetics is obtained. On the other hand, when the overall crystallization of the droplets is controlled by nucleation, very low Turnbull numbers are obtained (e.g., 0.1–0.01) with concomitant first-order kinetics. We also show how the nucleation step in the droplets can be skipped through the strategic use of self-nucleation. In the case of double crystalline polymer blends, the self-nucleation of the matrix can be used to study the surface nucleation of the droplets at the interface. The role of interfacial roughness in promoting droplet nucleation is also addressed, together with the addition of heterogeneous nucleating agents. Considering all the body of information, we demonstrate that studying the overall kinetics of different droplet dispersions can contribute to the fundamental understanding of polymer nucleation.

1. Introduction

When a bulk material is sub-divided into droplets or microdomains (MDs), changes in the overall crystallization of the material occur, that can advantageously be used to understand the basic mechanisms of nucleation and growth kinetics [1–3]. Bulk polymers typically nucleate on existing heterogeneities (catalytic debris or other impurities derived from their synthesis and processing).

Let's consider the preparation of a dispersion of a crystallizable polymer into an immiscible polymeric matrix. An asymmetric composition (e.g., 90/10 or 80/20) will generate a sea-island morphology with a large number of droplets. When the number of heterogeneities of the polymer to be dispersed is very low, and the number of resulting droplets is several orders of magnitude larger than the available heterogeneities, the droplets will be essentially heterogeneity-free (statistically speaking). In such a case, droplets tend to nucleate at the interphase or homogeneously in a single crystallization event. This single exothermic event usually occurs at a much larger undercooling than that at which the bulk polymer crystallization takes place. If the droplets nucleate homogeneously, then the crystallization occurs at very large undercooling, typically close to the glass transition temperature of the droplets.

If, on the other hand, the heterogeneity density in the bulk polymer is comparable to the number of droplets into which the polymer is

* Corresponding author. Polymat and Department of Polymers and Advanced Materials: Physics, Chemistry and Technology, Faculty of Chemistry, University of the Basque Country UPV/EHU, Paseo Manuel de Lardizabal 3, 20018, Donostia-San Sebastián, Spain.
** Corresponding author.
E-mail addresses: alejandrojesus.muller@ehu.es (A.J. Müller), dario.cavallo@unige.it (D. Cavallo).

https://doi.org/10.1016/j.polymer.2022.125514
Received 2 August 2022; Received in revised form 9 November 2022; Accepted 9 November 2022
Available online 19 November 2022

dispersed in an immiscible matrix, then a fractionated crystallization process develops. This is shown with a hypothetical polymer blend in Fig. 1 that, for illustrating purposes, we can consider as an amorphous atactic polystyrene matrix (aPS) and dispersed crystallizable isotactic polypropylene (PP) droplets in an 80/20 wt%/wt% composition.

Fig. 1, top left, shows the bulk PP containing nucleating heterogeneities with different efficiencies of nucleation. Impurity A is much more efficient than impurity B, i.e., it offers to the PP chains a lower heterogeneous nucleation free energy barrier (this can be due to its chemical nature, interactions with PP, epitaxial crystal structure match and other effects, such as size). When the PP is cooled from the melt, it will nucleate at lower undercooling on type A heterogeneity, triggering the appearance and growth of spherulites. Usually, type A impurities are present in sufficient quantity; therefore, the undercooled PP melt will be transformed to the semi-crystalline state (all spherulites grow and impinge on one another) before type B impurities can have a chance to nucleate at higher undercooling. The crystallization process of bulk PP occurs in a single high-temperature crystallization exotherm typically recorded during a non-isothermal DSC cooling scan from the melt (e.g., Fig. 1, bottom left).

When the crystallizing bulk PP is dispersed into numerous droplets within the aPS matrix, fractionated crystallization can appear if the number of droplets is of the same order of magnitude as the number of nucleating heterogeneities contained in the bulk polymer (Fig. 1, top right). In this case, the A and B heterogeneities will be distributed among the existing droplets, leading to droplets with one or more types of heterogeneity or clean droplets. Please note that some heterogeneities could also migrate to the matrix (during the blending process), and they are wasted in that case.

Fig. 1, bottom right, illustrates how the crystallization of PP (now in droplets) is split into four separate exotherms. As the crystallization of each droplet is independent, since droplets are well dispersed and thus separated from each other, each crystallization exotherm can be attributed to the crystallization of different droplet populations, each one with a different nucleation mechanism. The first droplet population to crystallize upon cooling from the melt is that containing the most active heterogeneities (i.e., type A). This population crystallizes at low undercooling at exactly the same crystallization temperature as PP in bulk. The second droplet population, crystallizing at lower undercoolings, is that containing type B heterogeneities. The undercooling increases as the nucleation efficiency decreases or as the energy barrier for nucleation increases.

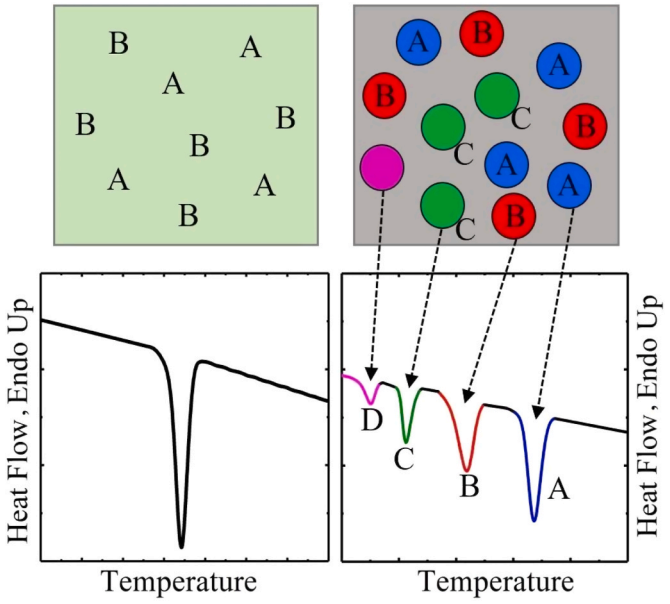

Fig. 1. Schematic illustration of the fractionated crystallization of PP droplets dispersed in an immiscible polystyrene matrix, as measured by DSC. In the present example, Bulk PP is assumed to contain two types of heterogeneities (A and B), as shown on the left. The DSC cooling scan for this bulk PP is reported on the left-hand side DSC curve. The same PP is dispersed into many droplets (top, right) inside a PS matrix, where each color represents a possible nucleation modality: blue, impurity A; red, impurity B; green, matrix interface (impurity-free droplets); purple, homogeneous nucleation (impurity-free droplets). The right DSC curve (bottom, right) shows the corresponding cooling scan where multiple crystallization exotherms are presented. Adapted with permission from ref. 3. (For interpretation of the references to color in this figure legend, the reader is referred to the Web version of this article.)

Further cooling of the sample causes the crystallization of the two last droplet populations. These are constituted by heterogeneity-free droplets. These droplets can crystallize at the interface (denoted by the letter C in Fig. 1, right) with the PS matrix (i.e., with a surface-induced nucleation mechanism) or homogeneously within the volume of the droplets (denoted by the letter D). Homogeneous nucleation occurs at very large undercooling, as required by the large energy barrier that needs to be surmounted to create a primary nucleus (i.e., the formation of a nucleus inside the droplet volume implies the creation of six new surfaces, an energetically costly process). These last two types of nucleation possibilities, surface-nucleation, and homogenous nucleation are difficult to distinguish by DSC and are not often occurring at the same time; they are represented in Fig. 1 to have, in one example, all types of nucleation modalities of droplets. The distinction between these two modes of clean droplet nucleation is often made empirically, as homogeneous nucleation is the one occurring very close to T_g, or quantitatively, by determining the domain size dependence of the nucleation rate (surface versus volume) [4].

Typically, bulk PP can contain approximately 10^6 active type A heterogeneities per cubic centimeter. If the blends are prepared with a compatibilizer that decreases droplet size and increases the number density of heterogeneities to values above $10^9/cm^3$, then the blend will contain an overwhelming majority of clean droplets, and exotherms A, B, and C will typically disappear, leaving only a large exotherm D, where exclusive homogeneously nucleated droplets crystallize [2].

Polymer solidification occurs via a two-step process. First, the material nucleates, and then once stable nuclei are produced, crystals grow [5,6]. In a bulk polymer, it is relatively simple to study separately primary nucleation and growth by employing a Polarized Light Optical Microscope (PLOM). However, if the nucleation rate is too high and the resulting nucleation density is too large, it may prove impossible to follow crystal growth by PLOM. Differential Scanning Calorimetry (DSC) can be operated under isothermal conditions, and the overall crystallization kinetics can be obtained for most crystallizable polymers. Furthermore, DSC allows measuring the overall crystallization of dispersed droplets.

To quantify the order of the resulting overall crystallization kinetics determined by DSC, the Johnson-Melh-Avrami-Kolmogorov model is commonly employed [7–12], also known as the Avrami model. The Avrami equation can be written as [11,13].

$$1 - V_c(t - t_0) = exp\ (-K(t - t_0)^n) \quad (1)$$

where $V_c(t)$ is the relative volumetric transformed fraction at time t, K the overall crystallization rate constant (i.e., nucleation + growth), t_0 is the incubation or induction time, and n the Avrami index.

Müller et al. [14,15] consider that the value of n can be expressed as:

$$n = n_{gD} + n_n \quad (2)$$

where n_{gD} is the dimensionality of the growing crystals and n_n the time dependence of the nucleation. The n_{gD} values can only be integer numbers, 1, 2, and 3, corresponding to one-, two- and three-dimensional crystallites or crystal superstructural units. For polymers, $n_{gD} = 2$ or 3, corresponding to either axialites (two-dimensional lamellar aggregates) or spherulites (three-dimensional lamellar superstructures). On the

other hand, n_n can have values between 0 and 1, where $n_n = 0$ corresponds to instantaneous nucleation, and $n_n = 1$ to sporadic nucleation.

The overall crystallization kinetics of bulk polymers is typically sigmoidal with kinetic orders of 2 and 3 (with a sigmoidal shape if, for instance, a plot of crystallization enthalpy versus time is represented). However, when an ensemble of isolated droplets is crystallized, the kinetics is typically dominated by nucleation, as the process of growth tends to be much faster. Hence, the slow step of the kinetics is droplet nucleation. Once a nucleus is formed inside a droplet, the time crystals take to grow, filling the small volume of a droplet can be many times faster than the nucleation time. Therefore, for highly dispersed isolated MDs, such as droplets, we can consider that n_{gD} tends to zero and $n = n_n$. Therefore, the overall crystallization for sporadically nucleated droplets is characterized by first-order kinetics since nucleation in the dispersed droplets occurs sporadically in time (i.e., $n = 1$).

In view of the above considerations, the overall crystallization kinetics order should be very different if the minor phase in a polymer blend is dispersed or co-continuous. In a co-continuous morphology, percolation of the crystallization phase occurs and isolated droplets will not be present. Percolation can spread crystallization via secondary nucleation; hence, fractionated crystallization will no longer be possible. Córdova et al. [16], studied reactively compatibilized polyethylene/polyamide, PE/PA6, blends. The functionalized polyethylene weight fraction and extrusion conditions can be carefully tailored for the production of blends with different morphology but similar composition. Polyamide sub-micron droplets were produced finely dispersed in the PE matrix on the one hand and with a co-continuous morphology on the other hand. Fig. 2 shows plots of their normalized crystallization enthalpy data points as a function of time with superimposed fits to the Avrami equation. TEM image insets show the blend morphology in Fig. 2. As expected, in the case of isolated droplet dispersions, the Avrami index is close to 1 (0.91) as the overall kinetics is dominated by sporadic nucleation, while it is close to 3 (3.06) for the percolated PA6 phase, where the growth of instantaneously nucleated spherulites dominates the kinetics. In this latter case, a deviation of the fitting values from the experimental data can be seen, for conversions exceeding about 0.5. Deviations from the Avrami equation can be usually encountered in many polymeric materials beyond the primary crystallization range, please see ref. 13.

Even though in many cases, the overall crystallization of well-dispersed droplets is dominated by nucleation, we have shown that depending on droplet size and the relative kinetics of primary nucleation versus growth, it is also possible to find growth-dominated overall crystallization kinetics in droplet dispersions [17]. A detailed discussion of this relevant aspect of droplet crystallization together with experimental data will be presented in sections 2.1 and 2.4.

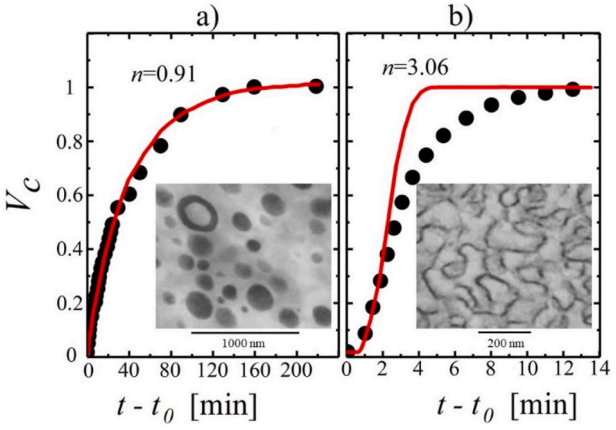

Fig. 2. Selected overall crystallization kinetics examples that follow DSC crystallization enthalpies as a function of time during the isothermal crystallization of the polyamide phase of immiscible PE/PA blends with either dispersed phase (left) or co-continuous (right) morphology. Red lines represent the fit to the Avrami equation (equation (1)). The insets are representative TEM images of the blend morphologies [3,16]. Adapted with permission from Elsevier. (For interpretation of the references to color in this figure legend, the reader is referred to the Web version of this article.)

There are many examples of fractionated crystallization in the literature (see a recent review by Sangroniz et al. [3] and references therein). It has been obtained in droplet dispersions [18–20], polymer blends [1–3,21–25], polymer multilayer films [26,27], block copolymers [15,21,28–31], and polymers infiltrated within alumina nanopores [21,32,33]. In this Feature Article, we will deal exclusively with polymer blends, as we are interested in exploring how droplet dispersions can be used to study nucleation and growth mechanisms in polymer crystallization by combining non-isothermal with isothermal crystallization and self-nucleation studies.

2. Nucleation modalities of semicrystalline droplets in immiscible blends

2.1. Self-nucleation of droplets in immiscible blends

The self-nucleation thermal protocol initially devised for solution-crystallized polymers [34] and later adapted to bulk-polymers crystallized in a differential scanning calorimeter [35], aims at producing a significant enhancement in the number of nuclei of the material by preserving a "memory" of the previous crystalline state of the sample. In the following, the procedure and the outcomes are briefly outlined, while the interested reader is addressed to recent reviews to go into more details on the phenomenon [36,37].

The first step of the procedure consists in preparing a "standard crystalline state" by crystallizing the sample from a melt temperature at which the thermal history is completely erased (e.g., a melting temperature 30 °C above the melting peak of the sample) in a controlled way (e.g., at a cooling rate of 10 °C/min). The sample crystallized in this way is then heated to the self-nucleation temperature (T_S) and kept there for a given time (e.g., 5 min). The outcome of the self-nucleation is judged by examining the following cooling and subsequent heating scans.

When the self-nucleation temperature is high enough, all the crystalline memory is erased, and the subsequent crystallization temperature shows no changes in comparison to that obtained by cooling from the "standard isotropic melt" (i.e., a fully relaxed isotropic melt, made up by randomly coiled polymer molecules). Such samples are said to be within *Domain I* or *melting Domain*.

Domain II is instead found when the T_S is high enough to melt most crystals but low enough to leave the so-called "self-nuclei". Their effect on re-crystallization from T_S can be highlighted by an increase in the crystallization temperature with respect to that in standard crystallization conditions (i.e., from *Domain I*). Upon heating the re-crystallized sample, no changes in the melting behaviour in comparison with *Domain I* are found since the T_S temperature is too high to cause meaningful annealing (and thus lamellar thickening) of the polymer crystals. The *self-nucleation Domain*, or *Domain II*, can be further subdivided into two regions, i.e., *Domain IIa* (at higher temperatures) and *Domain IIb* (at lower temperatures). In *Domain IIa*, also called *melt-memory Domain*, the sample is fully molten; thus, active self-nuclei must arise from regions in the melt where inter-segmental interactions have survived [36,38–42]. In *Domain IIb*, or *self-seeding Domain*, T_S is too low to melt all the crystals, and thus self-nuclei are constituted by small crystal fragments that act as ideal nucleation sites (i.e., self-seeds) for the crystallizing polymer.

Eventually, when the self-nucleation temperature is further lowered, *Domain III* or *self-nucleation and annealing Domain* is entered. In this temperature *Domain*, the unmolten part of the crystals anneals and thickens, as revealed by the final heating scan after re-crystallization, which shows a second melting endotherm at higher temperatures with respect to the main melting peak.

When the self-nucleation protocol is applied to the droplet phase in immiscible polymer blends, the typical fractionated crystallization behaviour (see Section 1) is altered due to the injection of self-nuclei in otherwise nuclei-free droplets [3]. For example, the PP minor component of an LLDPE/PP 80/20 blend was self-nucleated at the ideal T_S (i.e., the lowest in *Domain II)* by Müller et al. [43,44] The crystallization of the two components, which was overlapped in the blend due to fractionated crystallization of the PP phase, was thus resolved, with PP droplets increasing their nucleation temperature up to values characteristic of the self-nucleated bulk polymer phase. In another case, PP droplets dispersed in a polystyrene (PS) matrix showed up to 4 distinct fractionated crystallization peaks. The three exotherms occurring at higher temperatures were due to the presence of three nucleating heterogeneities with different efficiencies. The lowest temperature exotherm was produced by the crystallization of impurity-free droplets which crystallize at the highest undercooling [2]. When this sample is self-nucleated at $T_{S,ideal}$, a single crystallization exotherm is obtained at temperatures corresponding to that of the self-nucleated neat PP. These examples demonstrate that, as discussed in Section 1 (see Fig. 1), fractionated crystallization is due to the lack of the most active nucleating heterogeneities inside the droplets and can be efficiently eliminated if enough nuclei are injected into each of the droplets, for instance via self-nucleation or heterogeneous nucleation (see Section 2.4, further on).

In the following, based on our recent work [17], we will discuss in detail the effect of self-nucleation temperature on the non-isothermal and isothermal crystallization processes of PP droplets dispersed in a PS matrix. Fig. 3 shows representative examples of DSC cooling curves for 85/15 wt%/wt% PS/PP blends from different PP self-nucleation temperatures. Crystallization from the isotropic melt (T_S = 164 °C, *Domain I*) results in two fractionated crystallization peaks located at about 100 and 70 °C, with the latter, possibly due to the nucleation of the droplets on the PS surface, being the largest. *Domain II* is entered when the self-nucleation temperature is lowered by only one degree (T_S = 163 °C, see Fig. 4). In fact, the lower temperature exotherm (at 70 °C) disappears while the area of the higher temperature peak (at 100 °C) increases its value, as a consequence of the larger fraction of efficiently nucleated droplets (thanks to the applied self-nucleation or self-nuclei injection to the originally lower temperature crystallizing fraction).

On further lowering T_S, a new fractionated crystallization peak appears at even higher temperatures (i.e., about 120 °C), and its enthalpy becomes larger and larger, at the expense of the exothermic event at 100 °C, upon decreasing the self-nucleation temperature down to the beginning of *Domain III*. Thus more and more self-nuclei are being injected into the non-efficiently nucleated droplet population. By proceeding inside *Domain III*, the fraction of unmolten droplets becomes important, and the total crystallization enthalpy diminishes. The recorded change of fractionated crystallization behaviour of PP droplets in a PS matrix with self-nucleation is thus in agreement with the literature [2].

For what concerns isothermal crystallization, as learned in Section 1, isolated droplets generally crystallize independently from each other and sporadically in time, giving rise to first-order solidification kinetics. The crystalline volume fraction for PP droplets in a PS matrix, self-nucleated at $T_{S,ideal}$, and crystallized isothermally at 146 °C, is reported in Fig. 4 as a function of crystallization time. As evident from the trend of the fitting line, an Avrami exponent close to 3 is obtained, indicating sigmoidal crystallization kinetics, at variance with droplets cooled from a *Domain I* melt that display an exponent close to unity [17].

The sigmoidal crystallization kinetics is consistent with the growth of predetermined nuclei as 3-D spherulites, even though the droplet size is limited to a few micrometers. Remarkably, when self-nucleation is

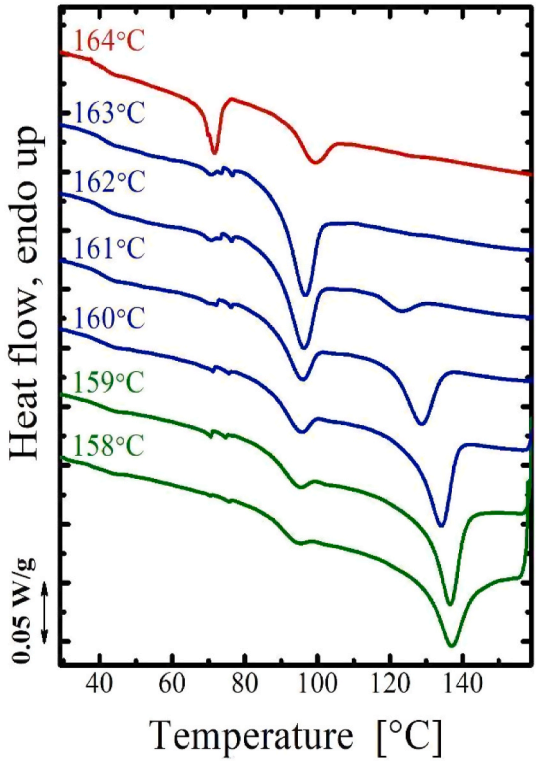

Fig. 3. Selected DSC cooling scans from the indicated T_s temperatures for the neat 85/15 wt%/wt% PS/PP blend. The different colors of the curves represent the three *SN* domains: *domain I* (red), *domain II* (blue), and *domain III* (green).[17]Adapted with permission from ACS publications. (For interpretation of the references to color in this figure legend, the reader is referred to the Web version of this article.)

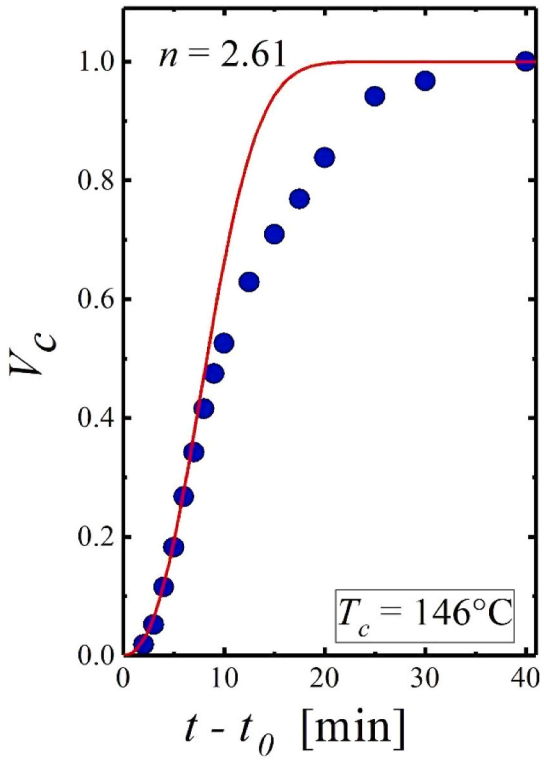

Fig. 4. Evolution of the crystalline volume fraction as a function of time for the PP droplets in the 85/15 wt%/wt% PS/PP blend, *SN* at T_s 160 °C (*Domain II*). The red line refers to the data fitting using the Avrami equation [17]. Adapted with permission from ACS publications. (For interpretation of the references to color in this figure legend, the reader is referred to the Web version of this article.)

performed at the ideal temperature, most of the droplets are efficiently and instantaneously nucleated, and thus the overall crystallization kinetics is dominated by the crystal growth step. This aspect will be discussed in detail in the following by analysing the undercooling dependence of the spherulitic growth rate and of the overall crystallization rate of PP droplets self-nucleated at various temperatures (see Fig. 5).

The growth rate data of polymer crystals as a function of undercooling are well described by the classical Lauritzen and Hoffman theory [45,46], according to which it is found that:

$$Log\ G = Log\ G_0 - \frac{U^*}{2.303\ R\ (T_C - T_\infty)} - \frac{K_g}{2.303\ T_C \Delta T\ f} \quad (3)$$

where G_0 is a growth rate constant, R is the gas constant, T_∞ is the temperature at which polymer segmental motion stops, U^* is the activation energy for the diffusion of crystallizing segments across the phase interface, ΔT is the undercooling ($=Tm^0 - Tc$), Tc is the crystallization temperature, and f is a temperature correction factor ($=2Tc/(Tc + Tm^0)$). K_g is the nucleation constant, proportional to the energy barrier for secondary nucleation.

Besides being derived for crystal growth, the Lauritzen and Hoffman theory has been commonly employed to fit DSC data of overall crystallization kinetics [13,47–50]. In the latter case, the energy barrier obtained from the fit is an "apparent" K_g (i.e., K_g^t) which contains contributions from both primary nucleation and growth. Lorenzo et al. have evaluated such contributions for various polymers crystallized by varying the self-nucleation temperature [51]. Their results showed that when self-nucleation is carried out at $T_{S,ideal}$, primary nucleation is completely accomplished within the self-nucleation step; thus, the overall crystallization rate measured via DSC contains information on growth rate only.

In Fig. 5, the reciprocal of the PP droplets half-crystallization time, which is proportional to the overall crystallization rate, is used in place of the growth rate in the linearized form of equation (3). The data refer to isothermal crystallization experiments performed on cooling from the indicated T_S, and the values of the growth rate measured by polarized optical microscopy are added for the sake of comparison. The overall free energy barrier for crystallization, K_g^t, is derived from the slope of the fitting lines, while the growth rate data provide the secondary nucleation energy barrier, K_g. Remarkably, when the ideal self-nucleation temperature (160 °C) is employed, the slope of the line fitting the overall crystallization kinetics is identical to the one related to crystal

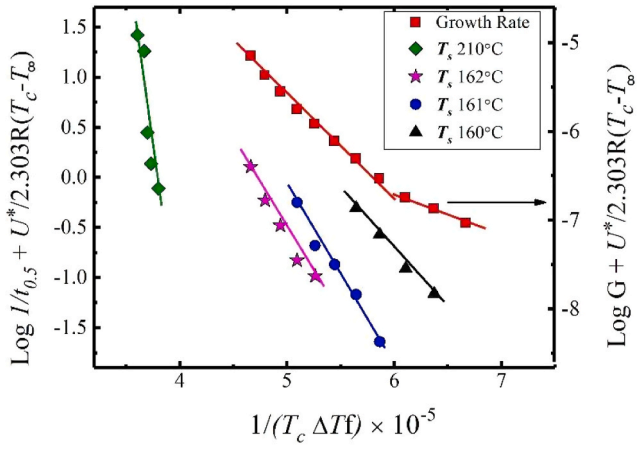

Fig. 5. Lauritzen and Hoffman plots for the DSC-determined overall crystallization rate (in the form of the reciprocal of the half-crystallization time) of neat and self-nucleated PP droplets and for polarized light optical microscopy determined spherulitic growth rate data for the bulk PP [17]. Solid lines are fits to the theoretical model (equation (3)). Adapted with permission from ACS publications.

growth. As discussed in the literature [13,51], and in agreement with the measured sigmoidal crystallization kinetics (Avrami exponent close to three, see Fig. 4), this indicates that crystal growth is the rate-determining step of the overall crystallization kinetics, while the energy barrier for primary nucleation is negligible. Instead, with increasing T_S, K_g^t progressively increases. For instance, the value changes from 2.65x10 [5] K^2 at $T_{S,ideal}$ to 19.3x10 [5] K^2 when the sample is crystallized from *Domain I*. The increase in the free energy barrier for the overall crystallization at higher T_S reflects the growing importance of the primary nucleation step, since part of the droplets (or most of them) are not nucleated.

In conclusion, we have demonstrated that self-nucleated droplets crystallize differently with respect to droplets solidified from a homogeneous melt. In particular, the lower the self-nucleation temperature, the more the overall crystallization tends to be dominated by the crystal growth stage rather than by the nucleation step.

2.2. Surface nucleation of droplets in immiscible blends

As discussed in Section 1, impurity-free droplets solidify at large undercooling either via nucleation at the interface with the matrix or by homogeneous nucleation [3]. Distinguishing between the two nucleation modalities is not trivial. As an example, in the classical work of Cormia, the crystallization of polyethylene droplets suspended in an inert medium was claimed to occur via a homogenous nucleation mechanism at around 85 °C [18]. However, twenty years later, Keller and co-workers showed that higher or lower undercoolings could be achieved when polyethylene droplets are deposited on a glass slide, depending on the surface treatment or wetting liquid on the substrate [52]. This demonstrated that nucleation of PE droplets occurs via a surface-induced mechanism. To unambiguously discern between the two nucleation mechanisms, the scaling factor of nucleation rate with droplet size must be checked. In fact, the nucleation rate should be proportional to the volume or surface of the droplet for homogeneous and surface nucleation, respectively. This detailed investigation has been carried out by Dalnoki-Veress et al. on dewetted droplets of polyethylene oxide, which exhibit a dependence of the isothermal crystallization time on the squared or third power of the droplets' radius, based on the exact nature of the used substrate [4,53]. However, such a study has never been conducted on immiscible blends.

For blends of a semicrystalline dispersed droplet phase within an amorphous matrix, some claims of nucleation occurring at the interface have been made [24,54]. For example, PP was mixed with PS, PMMA, and PC, while in the first two matrices, a single fractionated crystallization peak at 40 °C was observed, for PC/PP blends, the majority of the droplets crystallized at around 85 °C [54]. However, the possibility of impurity migration between the blend components (from the matrix to the droplet phase), and hence nucleation of the dispersed phase on different transferred impurities, cannot be safely ruled out. In double semicrystalline blends of PP dispersed in PA-6, the nucleation of the droplet phase at the interface was proposed, as judged by the increased crystallization temperature in the blend with respect to the bulk PP and by the disappearance of such an effect in the presence of some compatibilizers [55].

Recently, we proposed an approach to gain clear-cut evidence of surface-induced crystallization, which is applicable to dual semicrystalline immiscible blends with droplet morphology [56]. The method is based on the exploration of the correlation between the crystallization of the matrix phase, varied by means of the self-nucleation process and that of the dispersed phase. At first, the usefulness of the strategy is tested with blends of HDPE droplets in an PP matrix, a pair of polymers that are likely to exhibit surface-induced crystallization due to the known occurrence of polymer-polymer epitaxy between them [57–61]. The epitaxial nucleation of HDPE onto an oriented PP substrate has been extensively investigated in the literature: it is known that PE chains crystallize with an angle of 50° with

respect to the PP chain axis, because of the alignment of the zig-zag PE chain along rows of methyl groups of PP, with 0.5 nm intermolecular distances for a chain-row match [57]. Thus, the epitaxy can only occur if a particular geometrical relationship between PP and PE lamellar thickness is satisfied [59].

Thanks to our approach of matrix self-nucleation, the knowledge of surface-induced nucleation of PE on PP can be confirmed and extended to the domain of polymer blends with droplet-in-matrix morphology. The main results are discussed below.

Fig. 6a shows the cooling curves from the different indicated PP self-nucleation temperatures for a blend with droplet morphology containing 30% HDPE in an PP matrix. The three self-nucleation *Domains* are indicated with the colors of the curves according to the scale proposed by Müller et al. [36]: red for *Domain I*, blue for *Domain II,* and green for *Domain III*. At the highest self-nucleation temperatures, the crystallization peaks of the two crystalline blend components are partially overlapped, with that of HDPE found at lower temperatures with respect to the one of PP, as judged by the relative area of the peaks. No change in the position of the two peaks is detected at temperatures within self-nucleation *Domain I.* However, when *Domain II* of PP is entered, the two crystallization peaks begin to be separated due to the remarkable increase in PP crystallization temperature. More importantly, an upward shift in the peak crystallization temperature of the HDPE droplet phase is also recorded. Such shift is small but well recognizable, and the increase also continues when PP self-nucleation temperatures are within *Domain III*.

The crystallization temperature of the PP matrix and of the dispersed HDPE droplet phase are reported in Fig. 6b as a function of the applied self-nucleation temperature for different blend compositions, always with droplet-in-matrix morphology. The different self-nucleation

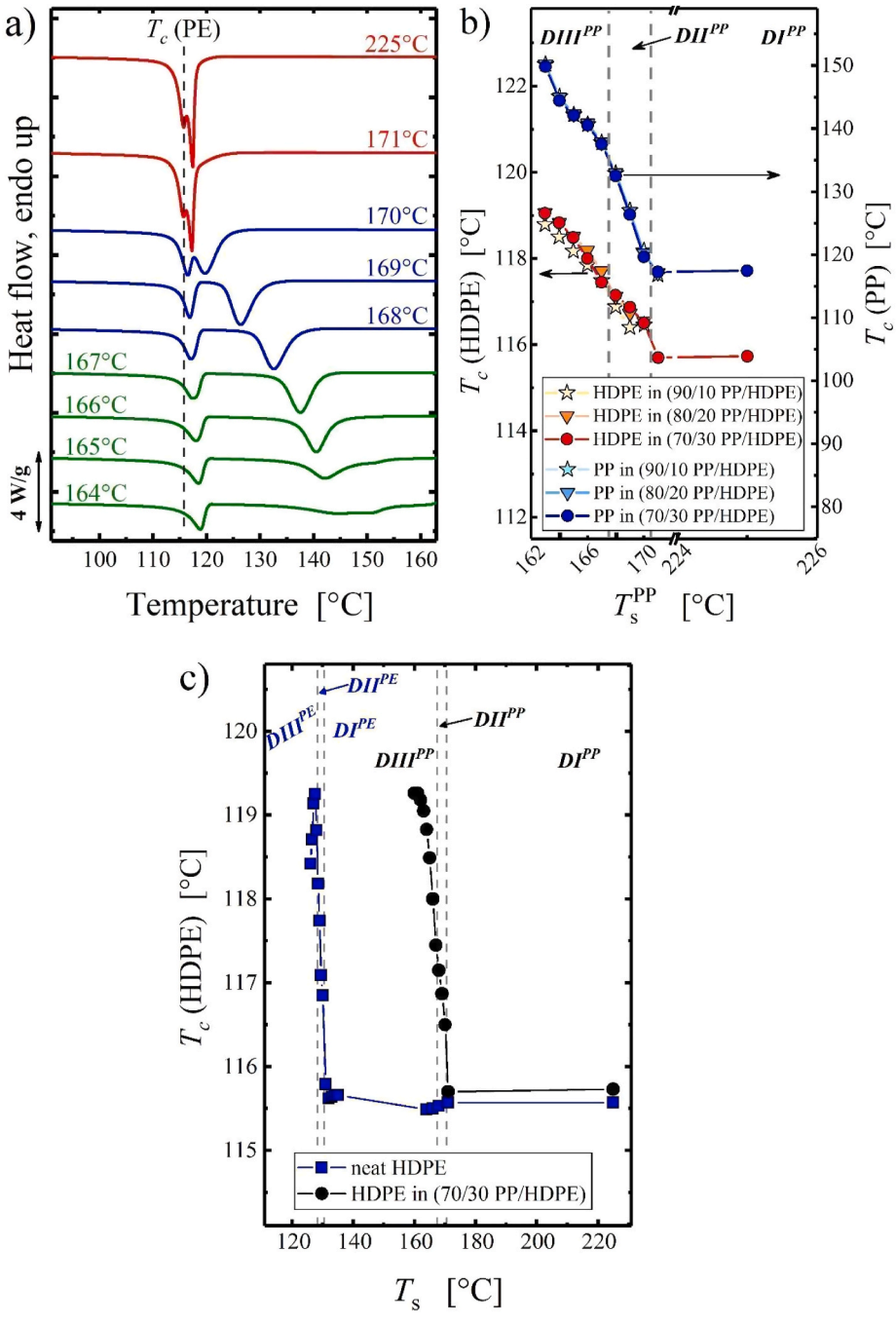

Fig. 6. (a) DSC cooling scans from the indicated T_s^{PP} values for the 70/30 wt%/wt% PP/HDPE blend. The different colors of the curves represent the three *SN* domains: *Domain I* (red), *Domain II* (blue), and *Domain III* (green). (b) T_c values for HDPE (left y-axis) and PP (right y-axis) in the 90/10 wt%/wt% PP/HDPE, 80/20 wt%/wt% PP/HDPE, and 70/30 wt%/wt% PP/HDPE blends as a function of T_s^{PP}. (c) T_c variation as a function of T_s for the neat HDPE across the self-nucleation *Domains* of PP and PE (from 225 to 160 °C and from 140 to 125 °C, respectively) and for the 70/30 wt%/wt% PP/HDPE blend in the self-nucleation domains of PP only. The self-nucleation *Domains* of PP phase in the blend are reported in black color whereas the ones of HDPE are in blue color. The solid lines reported for each series are guides to the eye [56]. Adapted with permission from ACS publications. (For interpretation of the references to color in this figure legend, the reader is referred to the Web version of this article.)

domains are also indicated for the sake of discussion. As already grasped by Fig. 6a, neither of the phases show meaningful variations in the T_C for self-nucleation temperatures within PP *Domain I*. *Domain II* and *Domain III* show, as expected, a steep increase in the crystallization temperature of the PP matrix, which is paralleled by a substantial increase (up to 3 °C) of the HDPE droplets' T_C. The results are consistent as they are obtained for all the investigated blends. This correlation between the rise in matrix crystallization temperature and the increased crystallization kinetics of the droplet phase clearly points towards an interaction between the two components at the interface. In particular, the hypothesis is that the increased crystallization temperature of PP modifies the crystalline state of the matrix, i.e., by increasing the lamellar thickness, which in turn favours HDPE nucleation at the interface via an epitaxial mechanism.

Interestingly, this increase in the crystallization kinetics of HDPE occurs at self-nucleation temperatures that are well above those required to self-nucleate neat HDPE (see Fig. 6c). In fact, in neat HDPE, the crystallization temperature as a function of self-nucleation temperature is invariant down to below 130 °C, while in the blend, the nucleation effect is active already below 170 °C. Moreover, when the maximum increase in T_C for HDPE droplets is compared with neat HDPE self-nucleation, a nucleation efficiency [62] of around 140% can be calculated [56]. This indicates extremely efficient nucleation, higher than that achievable with the self-nuclei of the same material, a phenomenon termed "supernucleation" [63–65].

Another interesting observation about the results presented in Fig. 6c is that after self-nucleating the PP matrix, the PE droplets experience a much wider *Domain II*, which now includes *Domain IIa* (or the melt memory sub-*Domain*) [36,37] as opposed to neat HDPE or the PE component in the blend without self-nucleation of the PP matrix. The origin of this peculiar melt memory effect is the surface-nucleation capability of the self-nucleated PP lamellae at the blend interface on the HDPE droplets. A similar situation has been encountered in PS/HDPE blends (see Fig. 11 and its discussion below), where surface-induced nucleation also enlarges the *Domain II* of dispersed HDPE droplets.

SEM micrographs on etched samples were acquired to investigate the morphological details of this nucleation process of HDPE droplets on a PP matrix. In particular, Fig. 7 displays a magnification of the droplet-matrix interface of samples crystallized upon cooling from 225 °C (PP *Domain I,* panel a) or from 163 °C (PP *Domain III*, panel b). In general, the PE lamellar stacks are oriented in a direction perpendicular to the droplet/matrix interface. What should strike the attention is the remarkable difference in lamellar density at the interface in the two samples (Fig. 7a vs. Fig. 7b). It seems that when cooled from PP *Domain I*, a lower linear density of nucleation develops at the interface, while when a self-nucleation temperature within *Domain III* is chosen, a transcrystalline layer develops since the nucleation density at the interface is so high that impingement among the individual growth fronts occurs and growth proceeds perpendicular to the interface, at least up to a certain extent. In Fig. 7b it is also possible to distinguish the thickened PP matrix lamellae, which have a thickness comparable to those of PE at the interface. In summary, morphological analysis corroborates the hypothesis of nucleation at the interface in droplets of HDPE in a self-nucleated PP matrix.

To gain more insights in the mechanism of interfacial nucleation of HDPE droplets on the PP matrix, isothermal crystallization experiments have been performed. Due to the exceedingly low rate of heat released by the dispersed droplet freezing, an isothermal step crystallization protocol has been adopted [14,66]. Fig. 8a reports an enlarged view of the melting endotherms obtained after steps of different duration at one chosen isothermal T_C and focused on the temperature range of the PE droplet phase. The melting enthalpy of the peak progressively increases with time, indicating an increased fraction of solidifying droplets. Notably, the saturation of the crystallization process was not reached due to the known process of secondary crystallization and isothermal thickening of PE lamellae.

Fig. 8b shows the crystallization kinetics of PE droplets at the given crystallization temperature of 123 °C, but in contact with a PP matrix of different lamellar thickness (varied via selecting the self-nucleation temperature) is shown. The overall crystallization kinetics increases with decreasing the PP matrix self-nucleation temperature, thus moving from *Domain II* to further inside *Domain III*, in agreement with the non-isothermal crystallization data shown in Fig. 6b. As shown by the matrix melting traces and by small-angle X-ray scattering (SAXS) analysis on selected samples, the lamellar thickness of PP increases with lowering the self-nucleation temperature from 169 to 163 °C [56], thus supporting the hypothesis of enhanced surface nucleation of PE dispersed droplets on thicker PP matrix's lamellae.

As stated in the introduction, a clear indication of nucleation-controlled crystallization in an ensemble of droplet microdomains is the obtainment of first-order overall crystallization kinetics (or equivalently, an Avrami exponent equal to one). Thus, the Avrami fitting has been performed on crystallization data of HDPE droplets dispersed in an PP matrix. Some examples of the obtained fit of the experimental data at different crystallization temperatures are provided in Fig. 8c, for a blend containing 20 weight percent of HDPE phase. For all the crystallization conditions, a satisfactorily fit is obtained, with values of the Avrami exponent comprised between 0.8 and 1.2, thus in agreement with a first-order kinetic model of the overall crystallization kinetics. Next, the data are plotted in the linearized form of equation (4) below (which assumes an Avrami index $n = 1$) in Fig. 8d:

$$1 - \frac{X}{X_{max}} = exp\ (-IV(t - t_0)) \tag{4}$$

where X/X_{max} is the fraction of droplets already crystallized, I represents the average nucleation rate, and V is the droplet volume.

From the slope of the lines reported in the plot, the values of the

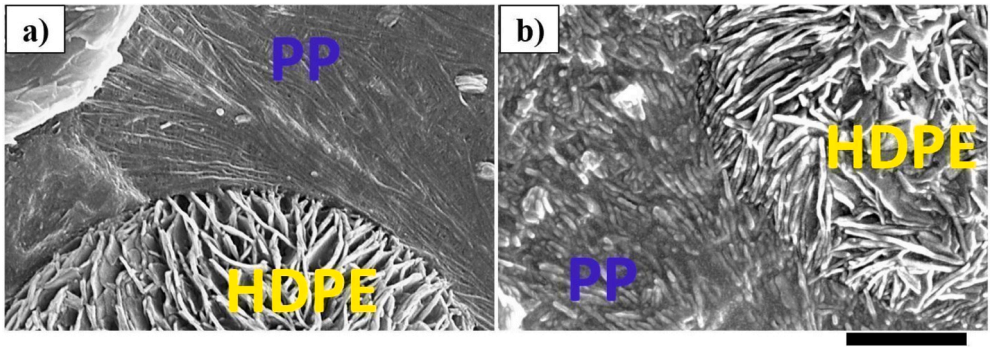

Fig. 7. SEM images of the 70/30 wt%/wt% PP/HDPE blend after cooling from (a) 225 °C (*Domain I* of PP phase) and (b) 163 °C (*Domain III* of PP phase) [56]. Scale bar is 1 μm. Adapted with permission from ACS publications.

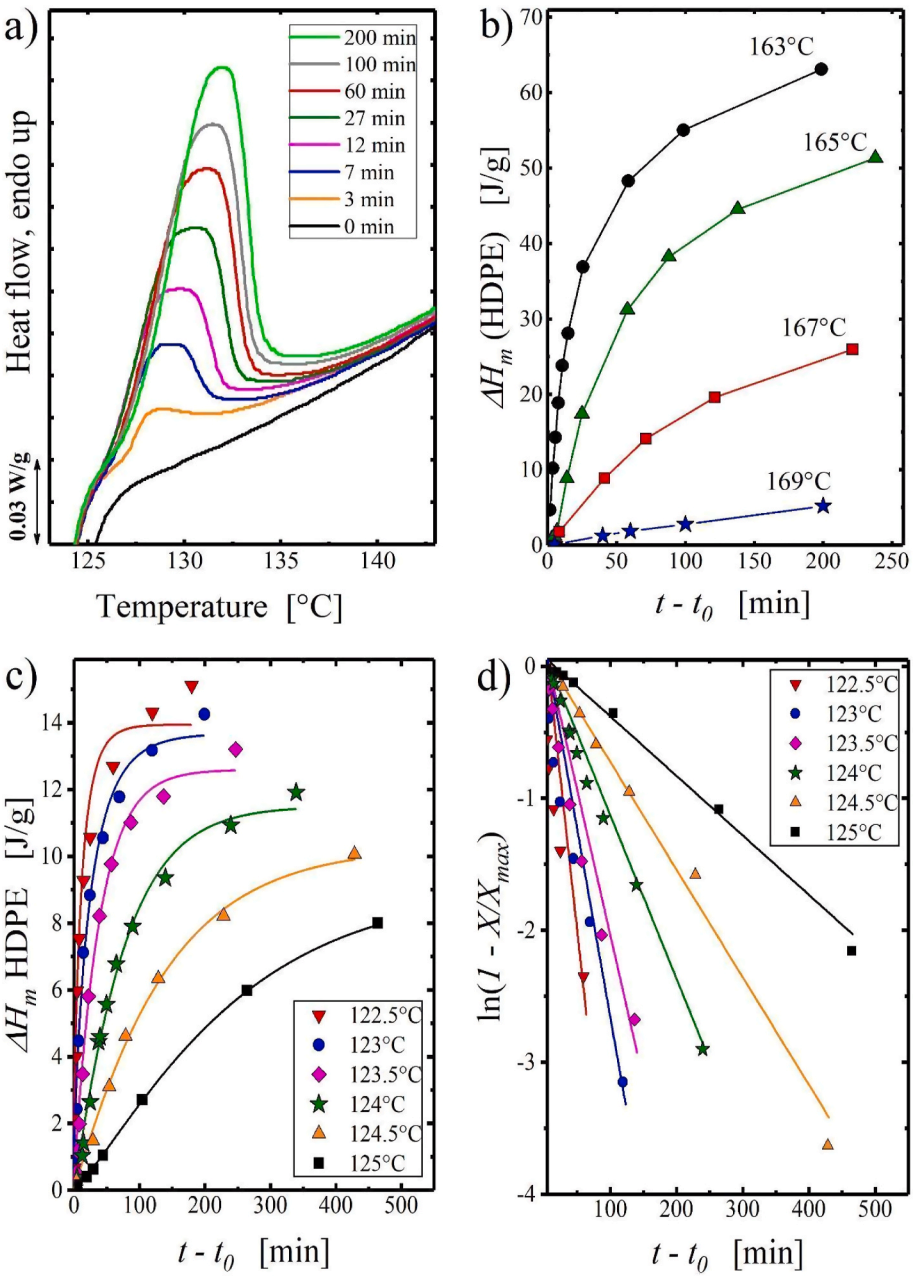

Fig. 8. (a) DSC final heating scans after annealing PP crystals at 163 °C and isothermal crystallization of HDPE at 123 °C for different times for the 90/10 wt %/wt% PP/HDPE blend. (b) Melting enthalpy of the HDPE phase ($\Delta H_{m\ HDPE}$) within 90/10 wt%/wt% PP/HDPE blend after self-nucleation/annealing of PP phase at the indicated *SN* temperatures and isothermal crystallization of the HDPE phase at 123 °C for different times. (c) Melting enthalpy of the HDPE phase ($\Delta H_{m\ HDPE}$) within 80/20 wt%/wt% PP/HDPE blend as a function of time during the isothermal crystallization measurements at the reported temperatures. The employed T_s^{PP} was 163 °C, and the solid lines are the result of Avrami model fitting. (d) Fitting of data (c) through the first-order kinetics model (equation (4)). Induction times are subtracted for the sake of clarity [56]. Adapted with permission from ACS publications.

nucleation rate (multiplied by the interfacial area, in the case of surface nucleation) can be directly derived. Knowing the value of the droplet surface area from morphological analysis, the rate of nucleation of HDPE droplet on the PP surface is finally calculated.

The derived heterogeneous nucleation rates can be analysed according to a classical nucleation model to attain information on the nucleation mechanism for the cases of different matrix lamellar thicknesses (i.e., different self-nucleation temperatures). The nucleation rate of the polymer on a substrate can be expressed in the linearized form as follows [67,68].

$$Log\ I = Log\ I_0 - \frac{U^*}{2.303\ R\ (T_C - T_\infty)} - \frac{16\sigma\sigma_e\Delta\sigma\ T_m^{0\,2}}{2.303k\ T_C(\Delta T\Delta hf)^2} \quad (5)$$

where I_0 is the temperature-independent frequency term, U^* is the activation energy related to the transport of chain segments across the phase boundary, R is the gas constant, T is the crystallization temperature, T_∞ is the temperature below which all motions associated with viscous flow cease, σ and σ_e are the lateral and basal surface free energies of the crystals, respectively, $\Delta\sigma$ is the interfacial free energy difference, Tm° is the equilibrium melting temperature, k is the Boltzmann constant, ΔT is the undercooling ($=T_m^\circ - T_C$), Δh_f is the heat of fusion per unit volume of crystal at T_m°, and f is a correcting factor ($=2T_C/(T_C + T_m^\circ)$), which accounts for the variations of the heat of fusion with temperature when a large range of supercooling is investigated.

Of particular interest are the two parameters obtained by fitting the experimental nucleation rate data with equation (5): I_0 and $\Delta\sigma$. The latter value corresponds to the difference in surface's free energy resulting from the replacement of a substrate/melt interface with a substrate/crystal plus a crystal/melt interface because of the formation of the first crystalline layer on the heterogeneous substrate. The magnitude of $\Delta\sigma$ is proportional to the free energy barrier for nucleation; thus, the lower its value, the faster and less temperature dependent the nucleation will be [17,69–72]. Instead, I_0, which depends on the molecular and transport properties of the nucleating polymer, represents a frequency of nucleation events per unit area (in the case of surface

nucleation) [17,67,68,72].

Fig. 9 shows the experimental data obtained on two series of HDPE droplets in contact with a PP matrix self-nucleated at temperatures of 167 °C (*Domain II*) and 163 °C (*Domain III*), are shown, together with the regression lines according to equation (5). The values of I_0 and $\Delta\sigma$ are extracted from the intercept and the slope of the fitting lines, respectively.

It is immediately evident that the $\Delta\sigma$ values obtained for the two systems are very close or identical, as expected, since the surface energies of the matrix and the nucleating polymer do not change among them. An average value of around 0.186 mJ/m^2 is obtained [56]. Such an extremely low value of interfacial free energy difference supports the epitaxial nucleation hypothesis, as similarly low $\Delta\sigma$ are obtained in the literature for systems in which epitaxy or lattice match between the nucleating polymer and the substrate is known [69–72]. The difference between the two ensembles of droplets, which leads to a difference in the nucleation kinetics, being higher for those in contact with the matrix self-nucleated at the lowest temperature, lays instead in the pre-exponential parameter I_0, i.e., the intercept of the fitting lines in Fig. 9. In particular, the values for the system with PP self-nucleation temperature of 163 °C are about 4 times larger than that for a self-nucleation temperature of 167 °C. This indicates a much larger number of available nucleation sites, in agreement with the morphological analysis presented in Fig. 7, which evidences a larger PE nucleation density at the interface in the respective case. All these data, together with some SAXS analysis which demonstrate that for surface nucleation of HDPE droplet on the surface of PP matrix to occur, a particular geometrical relationship between the two polymers' lamellar thickness must subsist, are strong indications that an epitaxial nucleation mechanism is also active for the HDPE droplets embedded in an PP matrix, in analogy with thin films of the same polymers [57–61].

A further proof that nucleation occurs at the interface in HDPE/PP blends with droplet-in-matrix morphology is provided by the use of an efficient compatibilizing agent. When a commercial ethylene-*ran*-methyl acrylate random copolymer is used as a compatibilizer, a reduction in the HDPE droplets size is observed, suggesting the localization of the third polymer at the interface between PP and HDPE. When the PP matrix is self-nucleated, the overall crystallization kinetics of the PE droplets in the blends containing the compatibilizer slightly decreases in comparison with the neat blend [73]. It is clear that compatibilizer addition can, in this case, somewhat interfere with the surface nucleation caused by the self-nucleated PP lamellae.

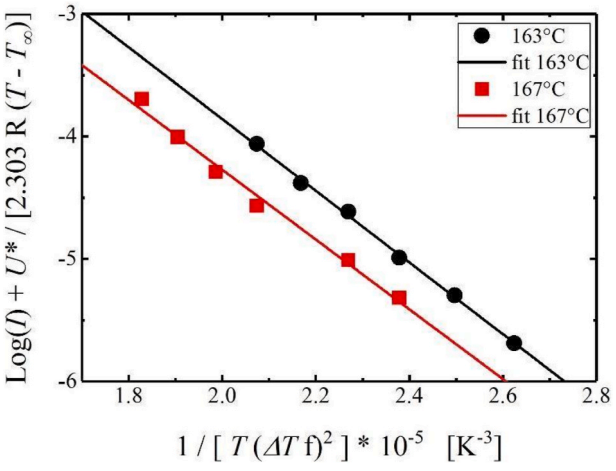

Fig. 9. Temperature dependence of the nucleation rate of HDPE droplets, in the 80/20 wt%/wt% PP/HDPE blend, according to equation (5) when the PP matrix is crystallized at two different T_s^{PP} values (163, 167 °C). The solid lines are the result of a linear fitting [56]. Adapted with permission from ACS publications.

The mentioned strategy, consisting of the self-nucleation of a matrix semicrystalline polymer to highlight the surface nucleation of the dispersed phase, is applicable to any polymer pair, provided that the melting temperature of the polymer dispersed into droplets is lower than the one of the matrix of the blend. As such, the method can conveniently be used to scout the surface nucleation effect of different matrices towards a given polymer. Recently, we extended the approach to binary blends of poly(1-butene) (PBu) droplets dispersed in PP and poly (vinylidene fluoride) (PVDF) matrices and to PCL droplets in various matrices (PP, HDPE, PBu, PVDF, and poly(butylene succinate) (PBS)) [74]. The results related to PCL droplets crystallization from the various self-nucleated matrices are reported in the following (see Fig. 10).

Fig. 10a compares the self-nucleation effect of the matrix on PCL droplet crystallization in the various blends with the results of neat PCL. No increase in PCL's T_C is detected for temperatures corresponding to *Domain I* of a given matrix. When the self-nucleation temperature is lowered below a certain threshold, a clear increase in PCL crystallization can be grasped, whose extent depends on the matrix considered. As discussed in the case of HDPE/PP blends, the enhancement of PCL droplet's nucleation kinetics is possibly due to the thickening of the lamellae of the matrix phase, which serves as a nucleating template. The data in Fig. 10a allow us to draw a nucleation efficiency scale among the different polymer surfaces (matrices). Considering the maximum in PCL *Tc* for each blend, the order found is: HDPE > PP > PB > PBS > PVDF. Notably, PCL/HDPE blends show an efficiency higher than 100%, similar to what occurs in the case of PP/HDPE. Also, in this case, the reason might be related to the occurrence of polymer-polymer epitaxy, already demonstrated by Yan et al. for this polymer pair in the form of thin films [75,76]. The second ranking of PP might be due to some degree of crystallographic matching with PCL, also reported in the literature [77]. Even in the absence of an epitaxial mechanism, the occurrence of droplet nucleation at the interface with the matrix is clearly demonstrated for all the investigated polymer pairs by means of the matrix's self-nucleation strategy. In the case of PCL/PVDF blends, although surface nucleation is still active, crystallization is occurring at temperatures lower than those recorded for the neat polymer. This result can only be due to the loss of some nucleating impurities by the PCL dispersed phase to the PVDF matrix during melt mixing.

A different perspective on the same surface-nucleation phenomenon is offered in Fig. 10b, where the T_C values for the PCL droplets are plotted as a function of the matrix T_C, varied via self-nucleation. For all the systems besides PCL/HDPE, the T_C of PCL droplets increases linearly with the T_C of the matrix, which in turn is indicative of an increased lamellar thickness of the substrate. As such, the observed correlation between the crystallization temperatures of the two phases suggests an increase in the droplet nucleation kinetics when in contact with thicker lamellae of the matrix polymer, as discussed above for the case of PP/HDPE blends. According to the template nucleation model [59,78] put forward for polymer-polymer nucleation, thicker lamellae of the substrate polymer enable easier nucleation of the second phase since crystallizing polymer chains segments suffer a lower free energy penalty due to the reduced contact with the substrate polymer's amorphous chain segments.

Our work on a variety of double semicrystalline blends with droplet-in-matrix morphology thus demonstrates that surface nucleation of the droplets is the major nucleation mechanism in such systems.

2.3. Interaction between self-nucleation and interfacial roughness in immiscible blends

In this section, the peculiar relationship between the roughness of the interface in immiscible blends and the self-nucleation behaviour of the dispersed droplets will be considered. In our recent work, we investigated the self-nucleation of HDPE droplets in their immiscible blends with either PS or Nylon 6 matrices [79]. Fig. 11a shows the DSC cooling scan after self-nucleation of the HDPE phase at different T_s. The

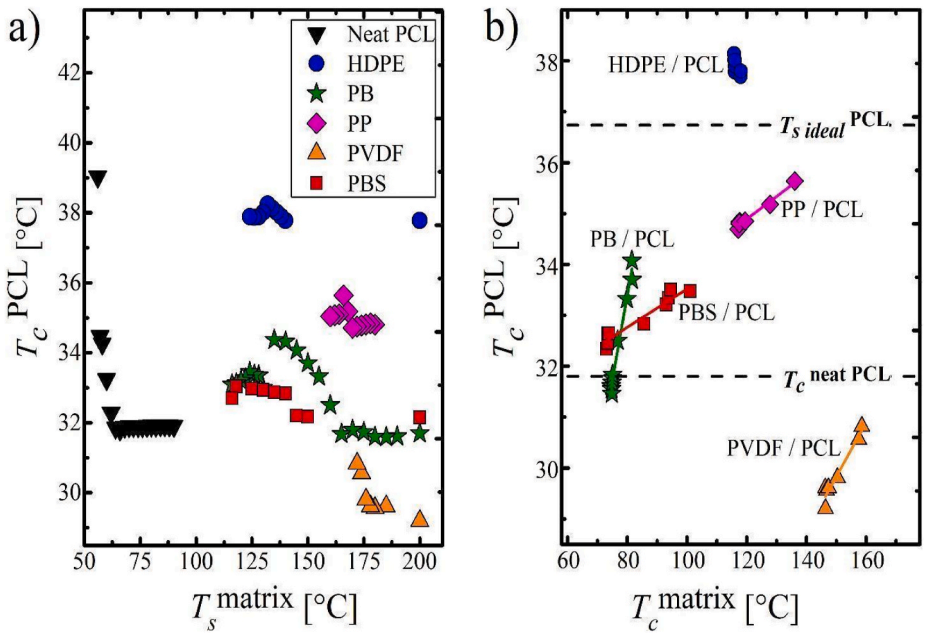

Fig. 10. (a) T_c values for PCL in the various PCL blends as a function of the matrix T_s. (b) T_c values for PCL dispersed phases in the corresponding blends as a function of matrix T_c. The horizontal lines report the crystallization temperature of neat and ideally self-nucleated PCL [74]. Adapted with permission from John Wiley & Sons Inc.

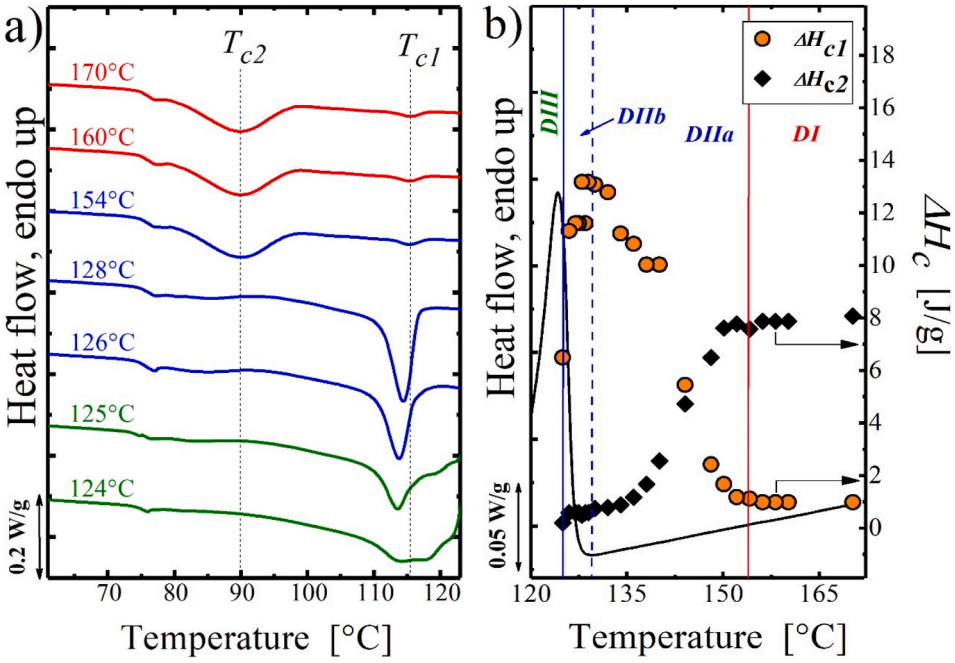

Fig. 11. (a) DSC cooling scans (at 10 °C/min) of the 90/10 wt%/wt% PS/HDPE blend after 5 min at the indicated T_s, (b) collection of ΔH_c as a function of the employed T_s (x-axis) superimposed on top of the standard DSC melting trace [79]. Adapted with permission from ACS publications.

crystallization enthalpies of the two main fractionated crystallization peaks are also reported as a function of T_s in Fig. 11b.

Considering the used neat HDPE, it crystallizes upon cooling from the melt in a single crystallization exotherm peaked at 116 °C and exhibited a conventional self-nucleation behaviour, where a very narrow *DII* (in the range 131–128.5 °C) is obtained. According to section 2.1, it is worth mentioning that neat HDPE in the present case exhibits only *self-seeding domain DIIb* (with a total absence of the *melt-memory Domain DIIa*). On the other hand, in the 90/10 PS/HDPE blend where HDPE is present in the form of droplets dispersed in the PS matrix, the HDPE minor phase exhibits fractionated crystallization where two main exotherms, T_{c1} and T_{c2}, peaked respectively at 115.7 °C and 90 °C are observed when the system is cooled from T_s higher than 154 °C (i.e., *DI*, see red curves in Fig. 11a). The results indicate the existence of droplets that crystallize at different degrees of undercooling. In terms of enthalpy, it should be noted that the crystallization enthalpy of the T_{c1} exotherm (i.e., ΔH_{c1}) is much lower than the one of the T_{c2} exotherm (i.e., ΔH_{c2}), indicating that only a small portion of droplets contains highly active heterogeneities, while most of the HDPE droplets are free of impurities or contain heterogeneities with lower activities and crystallize

at higher supercooling. By decreasing T_s to 154 °C, ΔH_{c1} starts to increase at the expense of the enthalpy of ΔH_{c2}, indicating the successful injection of additional self-nuclei inside some of the droplets (see Fig. 11 a,b). Further decrease of T_s down to 126 °C (i.e., $T_{s\ ideal}$) leads to an additional increase of ΔH_{c1} until ΔH_{c2} becomes practically negligible. The obtained results showed for the first time an HDPE phase with a very large *self-nucleation domain DII*, having a width of about 28 °C and an upper limit well above the equilibrium melting point of the polymer. The obtained *DII* includes both a very wide *melt-memory domain* (*DIIa*) and the *self-seeding domain* (*DIIb*). Any further decrease of T_s below 126 °C leads to the appearance of annealing, and thus we enter the *self-nucleation and annealing domain* (*DIII*) [79].

By extracting the HDPE phase from the 90/10 wt%/wt% PS/HDPE blend and employing the same *SN* thermal protocol on the recovered polyethylene phase, the authors demonstrated that when HDPE is not dispersed in the PS matrix, the polymer reverts to the original *SN* behavior of neat HDPE. To interpret the results, we refer to the work of Gałeski et al. [80], who reported severe surface roughening and meaningful changes at the interface after PP phase crystallization takes place in a PP/PE blend upon cooling from the melt. Considering these results, we attribute the observed peculiar *SN* behaviour in the blend to some surface roughness-induced nucleation originating from the PS/HDPE interface.

It is worth stressing that after cooling the system from the equilibrated melt, the HDPE droplets undergo crystallization, and their surface becomes rough. The shape of the formed lamellae will then be imprinted (forming a replica of the rugged surface topography) on the PS side of the interface during the subsequent heating scan to T_s, when the T_g of PS is exceeded and its viscosity is relatively low. We can then imagine that the obtained additional surface roughness can only be erased by heating the sample to a higher temperature (T_S in *Domain I*), where HDPE is fully molten, and the PS component is fluid enough to relax the interfacial asperities. For lower T_S, the rough topography of PS is retained because the viscosity of the polymer is too high and prevents interface relaxation. Obviously, the rough interface promotes HDPE nucleation during cooling from T_S, providing abundant surface-nucleation sites [4].

To verify the appearance of the PS/HDPE interface at different T_s, SEM and TEM analyses on the blends were performed. The micrographs were taken at room temperature after cooling from the different T_s. Fig. 12a and b shows results of the SEM micrographs of the cryogenically fractured surface of 90/10 wt%/wt% PS/HDPE blend self-nucleated at 170 °C and 132 °C, respectively. Results confirmed that the PS surface roughness and the interface state are clearly changed after changing the self-nucleation temperature. In fact, by employing a T_s of 170 °C (T_s within *DI*), the HDPE droplets reach an isotropic melt in parallel with the PS matrix having a very low viscosity; hence the surface of both HDPE and PS becomes fully relaxed, and the interface smoothens (Fig. 12a). On the other hand, when a T_s of 132 °C is applied, the interface between the HDPE phase and the PS matrix remains rough and deformed (because at this T_s, the PS matrix is not fluid enough to relax the interface and make it smooth). Consequently, due to such a rough interface, the HDPE phase exhibits enhanced surface nucleation and crystallization during the following cooling.

Fig. 12c and d shows TEM micrographs of the 90/10 wt%/wt% PS/HDPE blend after self-nucleation at 170 °C and 140 °C, respectively. Fig. 12d confirms the enhanced surface nucleation in which, by employing a T_s of 140 °C (a T_s at the lower temperature range of *DII,* see Fig. 12b), the crystallization of HDPE droplets tends to be controlled mainly by surface-induced nucleation (see arrows in Fig. 12d pointing to some PS/HDPE interface spots from which the nucleation initiated). The presented findings emphasize clearly that the employed T_s was able to

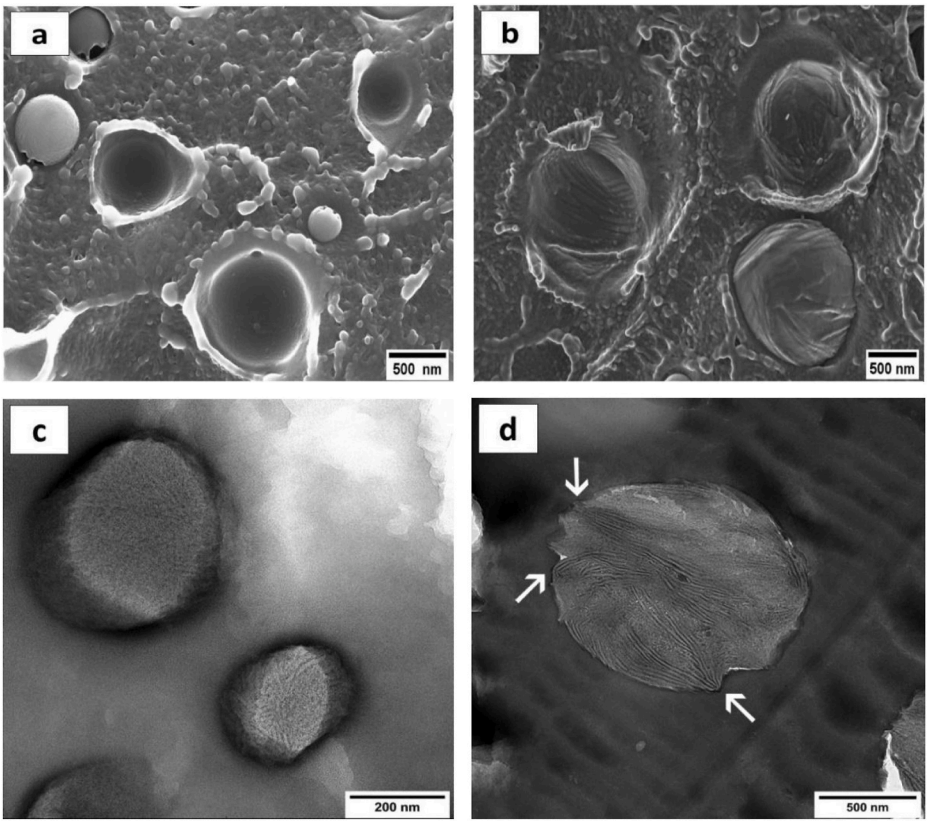

Fig. 12. (a,b) SEM micrographs and (c,d) TEM micrographs of the SN 90/10 wt%/wt% PS/HDPE blend; (a,c) SN at 170 °C, (b) SN at 132 °C, and (d) at 140 °C. The arrows show points from which some HDPE crystalline lamellae start. The applied thermal protocol before this SEM/TEM analysis is shown in Fig. S1 of [79]. Adapted with permission from ACS publications.

affect: (i) the roughness of the interface; (ii) the crystalline memory of the HDPE phase (also possibly due to the presence of some type of ordered polymer chains trapped inside the formed cavities and grooves at the PS/HDPE interface); (iii) the HDPE surface induced nucleation.

Moreover, Fenni et al. [79] investigated the *SN* behavior of the HDPE in a 90/10 wt%/wt% Nylon 6/HDPE blend. Results showed that also in the case of the Nylon 6 matrix, the HDPE phase exhibits a very strong melt-memory with an upper limit of *DII* at 160 °C. In this case, the enhanced melt memory was attributed to the surface roughness induced by Nylon 6 crystallization during the first cooling step of the *SN* thermal protocol, which in turn affects the blend interface and hence the overall *SN* behaviour. The obtained stronger melt memory and the enlarged self-nucleation *Domain* in the PS/HDPE phase were also observed in several other systems where other amorphous matrices were employed [79]. These findings allow to conclude that the observed strong melt-memory is a general effect associated with the presence of interface when HDPE is dispersed in another matrix, and that there can thus be an intriguing interplay between the self-nucleation of polymer droplets (section 2.1) and their surface-induced nucleation (section 2.2).

2.4. Heterogeneously nucleated droplets in immiscible blends

Droplets clean from naturally occurring nucleating impurities constitute an ideal system for studying heterogeneous nucleation effects. In fact, as recognized by Keller and co-workers [52], removing "background" nucleation sites in pure droplets provides a good baseline, against which the efficiency of an intentionally added nucleating agent can be probed with high sensitivity. Moreover, as shown in Section 1, isolated droplets display first-order overall crystallization kinetics (see Fig. 2), which in principle make the direct measurement of heterogeneous nucleation rate possible.

Two main methods for the study of heterogeneous nucleation by means of droplets crystallization can be found in the literature. The first requires the deposition (or the direct formation) of the droplets on the heterogeneous substrate, which has to be tested for its nucleation effect. The application of this method dates back to 1967, when Koutsky et al. deposited polyethylene droplets on different alkali halides cleaved surfaces, recording meaningful differences in the achievable undercooling [81]. More recently, Dalnoki-Veress et al. demonstrated that nucleation occurs at the surface in dewetted droplets of polyethylene on atactic polystyrene substrate and in poly(ethylene oxide) (PEO) on crystallized isotactic polystyrene [4,82]. The scaling of nucleation rates with the basal surface of the droplets was evidence of heterogeneous nucleation of the polymer on the given substrate. Finally, the heterogeneous nucleation of a highly oriented pyrolytic graphite substrate towards PEO was measured in a non-isothermal droplet crystallization experiment by Dolynchuk et al. [83]. An increase of about 11 °C in crystallization temperature was detected with respect to dewetted PEO droplets on atactic polystyrene, which are known to solidify via homogeneous nucleation [4,53].

The second method consists in using droplets incorporating the nucleating particle that needs to be tested for its efficiency. This strategy was first adopted by Perepezko et al. for metallic droplets [84]. They studied the nucleation of tin droplets inoculated with different chemical compounds, i.e., various oxides, sulphides, and tellurides. A difference in the undercooling achieved by the distinct compounds was found. Later, the approach revealed to be effective also for semicrystalline polymers droplets in immiscible blends. Santana and Müller showed that, while a PS/PP blend with droplet morphology exhibits fractionated crystallization behaviour (see Section 1), by adding a phthalocyanine blue pigment to the blend a single crystallization exotherm was found at a temperature higher than those of the bulk PP phase [85]. Baer et al. also studied droplets of PP in a PS matrix, but obtained via breakup of PP nanolayers. The droplets were nucleated with different soluble or solid heterogeneous nucleating agents or polymer additives [54,86–88]. Again, it was seen that the low-temperature exotherm, characteristic of the homogeneous nucleation process, disappears in favour of a high-temperature one with increasing nucleant's concentration, provided that the size of the PP droplet was commensurate to the size of the added particle.

It must be underlined that most of the above-mentioned works, while demonstrating the concept of using droplets crystallization to study heterogeneous nucleation, largely focused on non-isothermal measurement only. Recently we have carried out a detailed investigation, including isothermal heterogeneous nucleation rate measurements, on PP droplets nucleated with various additives and dispersed in an immiscible polystyrene matrix [17]. The key findings are summarized in the following.

Fig. 13 reports the effect of adding an increasing concentration of the nucleating agent sodium 2,2′-methylene bis-(4,6-di-tertbutylphenyl) phosphate), commercially named NA-11, on the fractionated crystallization of PP droplets in a PS matrix. When 0.1 wt% of nucleating agent is added, the DSC curves upon cooling from the melt of that system is basically identical to that of the neat PS/PP blend. One minor difference is found at around 50 °C where a small fractionated crystallization peak is found for the blend containing 0.1 wt% NA-11. This peak in PP blends is commonly attributed to a fraction of extremely small droplets which nucleate via homogeneous nucleation [54,85–88]. Its presence in the blend with NA-11 but not in the neat PS/PP system might be due to slight unintended differences in the preparation conditions, or to differences in the viscosity ratio of the components with the presence of the nucleating agent. It should be noted that the same amount of NA-11 added to bulk polypropylene evidences a nucleation effect with respect to the neat polymer. As such, we deduce that at this concentration, since no effect is recorded in the blend, either the number of NA-11 particles is insufficient to nucleate the large number of droplets, or that part of the nucleating agent is lost in the blending process, via transfer to the matrix phase [89].

When the NA-11 concentration is increased, the low crystallization exotherms (at approximately 70 and 100 °C) progressively disappear, in

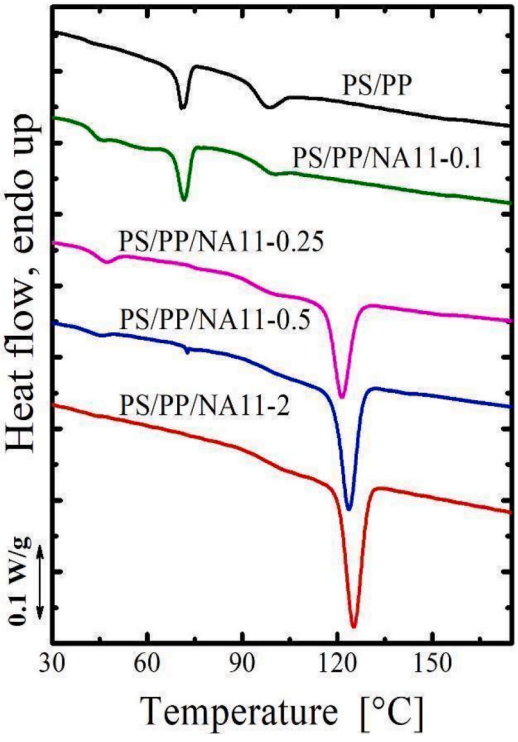

Fig. 13. DSC cooling curves of bulk PP and blends containing NA11 nucleating agent at the indicated composition in weight percentage [17]. Adapted with permission from ACS publications.

favour of a new high-temperature crystallization event located above 120 °C. The high-temperature peak continuously increases its area with the addition of more nucleating agent, indicating a larger amount of efficiently nucleated droplets and/or a faster crystallization kinetics due to a higher average number of nucleating seeds per droplet [90]. Moreover, for the highest amount of added NA-11, the homogeneous nucleation peak related to the fraction of smaller droplets also disappears, suggesting that the number of NA-11 particles is high enough to nucleate all the droplets in the system, in agreement with similar findings in the literature [86,88].

To demonstrate that nucleation is the rate-determining step also for heterogeneously nucleated droplets, analogously to neat droplets, we focused our attention on isothermal crystallization kinetics. Representative examples of the evolution of the crystalline volume fraction (according to the Avrami equation, see Section 1) with time for PP droplets nucleated with NA-11 or neat are shown in Fig. 14 a and b, respectively. It can be seen that the data are well described by the Avrami equation (continuous lines in Fig. 14 a and b), and the Avrami exponent can be easily appreciated by the slope of the linearized plot of the Avrami equation, reported in Fig. 14c.

For both systems, the Avrami exponent is close to 1, clearly indicating that the nucleation step dominates the overall crystallization. The remarkable finding is that even if efficient nucleating agents are added to the droplets, although the overall crystallization kinetics accelerate in comparison to that of the non-nucleated droplet, it remains nucleation controlled. The reason for this must be found in the reduced size of the droplets, which makes negligible the time for filling the droplet volume by crystal growth with respect to the nucleation time (even if the nucleating agent shortens the latter). On the contrary, droplets self-nucleated at $T_{s,ideal}$ display an Avrami exponent close to 3, representing growth-controlled crystallization (see Section 2.1). The linearized Avrami data of ideally self-nucleated droplets are added to Fig. 14c, for

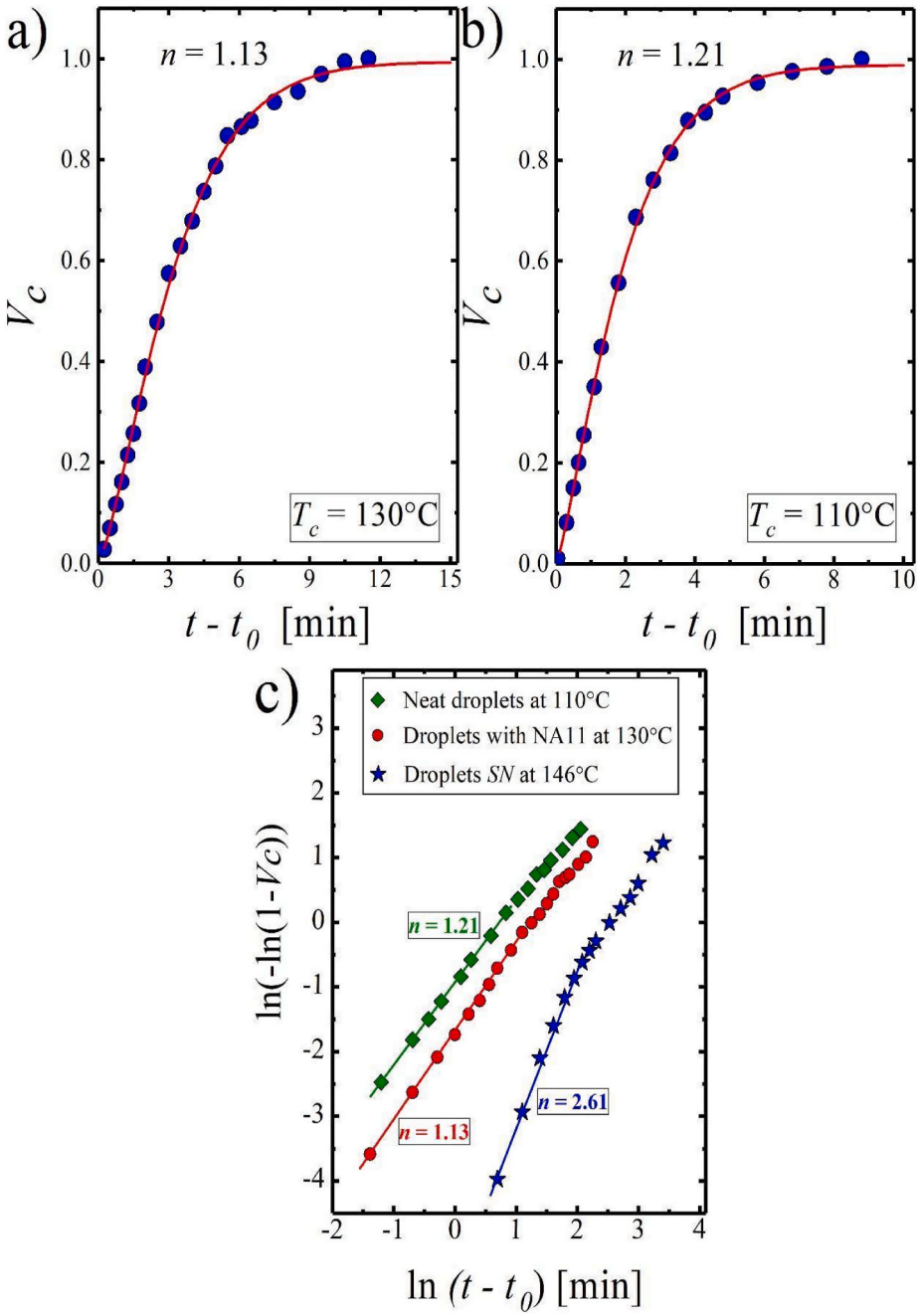

Fig. 14. (a,b) Evolution of the crystalline volume fraction as a function of effective crystallization time for the PS/PP/NA11–0.25 and self-nucleated PP droplets from T_s = 210 °C (*Domain I*), respectively. The red lines represent the fitting of the data with the Avrami equation. (c) Linearized Avrami plot of the crystallization data related to: PS/PP/NA11–0.25; self-nucleated PP droplets from T_s 160 °C (*Domain II*); self-nucleated PP droplets from T_s 210 °C (*Domain I*). The colored lines represent linear fittings in the conversion range 3–20%, from which the indicated values of Avrami index are obtained.[17]Adapted with permission from ACS publications. (For interpretation of the references to color in this figure legend, the reader is referred to the Web version of this article.)

the sake of comparison. As discussed in the respective section, in self-nucleated droplets, primary nucleation is accomplished practically instantaneously, so the rate-determining step has to be the crystal growth stage. The concept of the competition between growth and nucleation time scales inside a droplet of average size will be further discussed in detail in this section.

The values of the Avrami exponent obtained for the various systems, i.e., PP droplets in PS matrix self-nucleated at different temperatures and heterogeneously nucleated with the various nucleating agents, are reported in Fig. 15 for comparison. The data are clustered in two areas, between two and three (growth-controlled crystallization) or around one (nucleation-controlled crystallization). In particular, both the droplets self-nucleated from *Domain I* (see Section 2.1) and those nucleated with the different additives lay in the first-order kinetics region (Avrami exponent equal to one). However, a difference in the achievable undercooling for the two systems is observed, with heterogeneously nucleated droplets crystallizing at much higher temperatures than neat droplets cooled from *Domain I*, because in the latter nucleation probably occurs at the interface with the matrix, with a much higher interfacial free energy difference $\Delta\sigma$.

It is noteworthy that first-order kinetics can thus always be found when nucleation is the rate-determining step of the overall crystallization, i.e., in droplets that are homogeneously nucleated [53], laying on a nucleating substrate [81], or containing heterogeneous nucleants such as in this case [17].

On the contrary, PP droplets self-nucleated at temperatures within *Domain II* (see Section 2.1) display Avrami exponent comprised between two and three, characteristic of sigmoidal overall crystallization kinetics, controlled by two or three-dimensional crystal growth. The Avrami exponent and the achievable range of undercoolings increase with decreasing T_S. This is because for only partially self-nucleated droplets the contribution of primary nucleation to the overall crystallization kinetics becomes of importance (see Section 2.1). Therefore, a transition from sigmoidal to first-order crystallization kinetics is found when moving from $T_{S,ideal}$ to *Domain I* [17].

As shown by the analysis of the Avrami indexes, crystallization in droplets dispersed in a matrix in immiscible blends is not always controlled by nucleation, but growth can play a decisive role in determining the overall crystallization kinetics. To further understand this concept, a dimensionless number that compares the time scales for growth and nucleation inside the droplets can be employed [90]. The mean "growth time", t_G, i.e., the time required for a crystal growing inside a droplet of volume V to completely fill the domain, is given by:

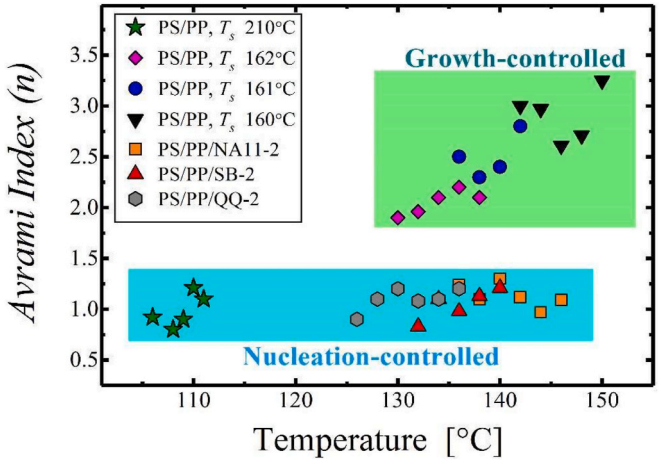

Fig. 15. Avrami indexes for neat PS/PP blends with different *SN* temperatures (T_s) and for 85/15 wt%/wt% PS/PP nucleating agents blends as a function of crystallization temperature (T_c).[17]Adapted with permission from ACS publications.

$$t_G = \frac{\sqrt[3]{V}}{G} \tag{6}$$

where G is the spherulitic growth rate at the given temperature. On the hand, the "nucleation time" t_N in a droplet of the same volume is given by:

$$t_N = \frac{1}{I \bullet V} \tag{7}$$

where I is the nucleation rate determined by equation (4) (see Section 2.2). The denominator of equation (7) is, in essence, the slope of the fitting lines of the plots analogous to those shown in Fig. 8d. When droplet systems show sigmoidal crystallization kinetics, e.g., for self-nucleated droplets, the half-crystallization time can be used instead of the "nucleation time", for testing the hypothesis of solidification controlled by nucleation in this case as well.

The ratio between the two above-defined times, i.e., growth time/nucleation time, is thus informative about which is the mechanism controlling the overall crystallization in the droplet. In particular, growth will dominate the crystallization process for values of this dimensionless number close to unity, while values much lower than one correspond to nucleation control. In the latter case, it can be assumed that a single nucleus will form in the droplet, and the growth proceeds fast enough so that the time for its occurrence can be neglected. We propose to name the ratio between mean growth and nucleation times (t_G/t_N) in a droplet system the "Turnbull number", in honour of the pioneering work of the scientist on droplet crystallization [18,19].

Values of this dimensionless number for two different droplet systems, namely PP droplets in a PS matrix and HDPE droplets in a PP matrix are reported in Fig. 16 a and b, respectively. In Fig. 16a, data for heterogeneously nucleated and self-nucleated droplets are displayed as a function of the isothermal crystallization temperature. Droplets self-nucleated at the ideal temperature display a ratio between growth and nucleation times close to unity, indicating growth-controlled solidification kinetics, in agreement with the measured sigmoidal trend of crystalline volume fraction with time (see section 2.1) and the consequent value of the Avrami exponent equal to three (Fig. 14 c and 15). On the other hand, for droplets nucleated with sodium benzoate or NA-11 and for neat droplets cooled from *Domain I,* the mean nucleation times are tens to hundreds of times longer than the time required to grow a crystal inside the whole droplet volume. This is clear-cut evidence for nucleation control in the overall crystallization, conforming to the measured first-order kinetics (Fig. 14 a and b and Fig. 15). Interestingly, the Turnbull number decreases with increasing *Tc* in these systems, meaning that the difference between growth and nucleation times gets wider as the undercooling decreases, as a consequence of steeper temperature dependence of the nucleation rate with respect to the growth rate.

A different situation is shown in Fig. 16b, which reports the data of neat and compatibilized PP/HDPE blends, where HDPE is the droplet phase. Remarkably, at higher undercoolings the overall crystallization rate of HDPE droplets can be measured directly and exhibits sigmoidal kinetics. Accordingly, the Turnbull number, t_G/t_N, is close to unity for both neat and compatibilized blends. This indicates that growth is the rate-limiting step of the overall crystallization in the HDPE droplets since the nucleation rate must be very high at these low crystallization temperatures. Higher crystallization temperatures are achieved by employing the self-nucleation of the matrix strategy outlined in Section 2.2. In this case, for all the investigated systems, nucleation times largely exceed the growth times inside the droplets, with the Turnbull number being smaller than 0.01. This drastic change in the Turnbull number with increasing crystallization temperature must be related to a different undercooling dependence of the nucleation and growth rates, with the latter being retarded much less than the former with increasing T_C.

Having demonstrated that PP droplets in immiscible blends can be

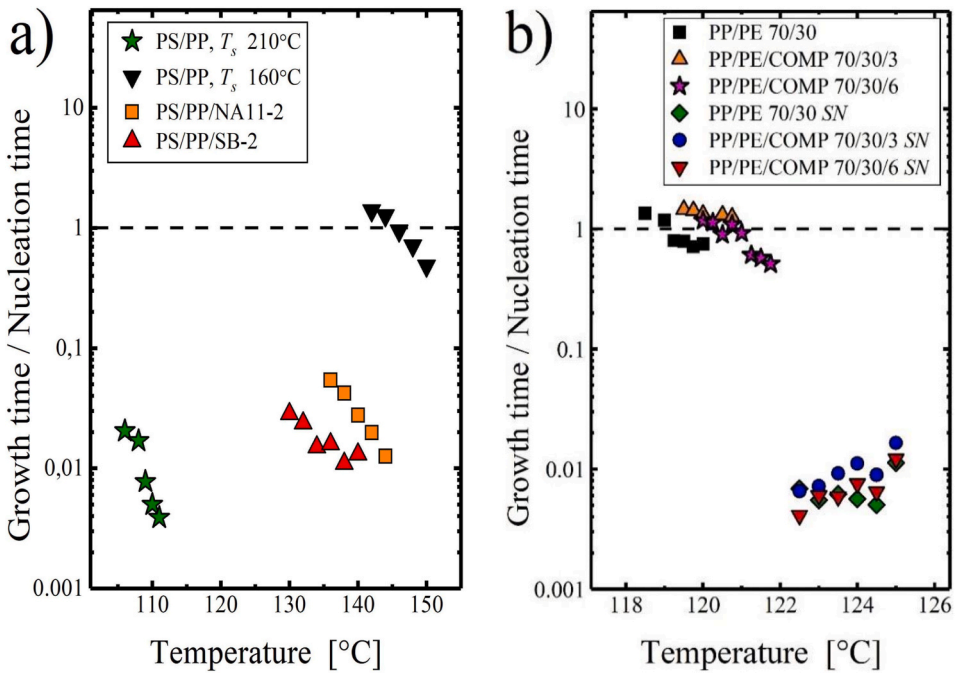

Fig. 16. Turnbull number (i.e., ratio between growth time and nucleation time) at different temperatures for (a) PP droplets for the indicated 85/15 wt%/wt% PS/PP systems [17], and (b) PE droplets in the mentioned PP/PE systems.[73]Adapted with permission from ACS publications and Elsevier.

heterogeneously nucleated [17], we turned our attention to the use of nucleating agents with dual nucleation ability, able to promote the formation of different PP polymorphic structures [91]. In particular, some heterogeneous nucleating agents are known for their ability to nucleate a metastable polymorph, called the β-phase [92–94], which is desirable because of better balanced mechanical properties compared to the usual α-phase. In our recent work, we adopted the developed droplet-in-matrix approach to study the heterogeneous nucleation behaviour of two such nucleating agents, namely Quinacridone Quinone (QQ) and N,N′-dicyclohexylterephthalamide (DCHT) [91].

A series of DSC melting curves obtained for different crystallization times, employing the isothermal step crystallization method [14,66], for PP droplets nucleated with QQ and dispersed in a PS matrix, are displayed in Fig. 17a. Two melting peaks at ca. 143–147 °C and 152–155 °C are distinguished. Based on detailed calorimetric and structural analysis [91] they are attributed to the melting of β- and α-crystals, respectively. As judged by the relative fraction of the two peak areas, a comparable amount of the two phases is generated during crystallization. Interestingly, the two phases show distinct nucleation kinetics, with the quantity of α-phase being larger than that of β-phase at the beginning of the crystallization, while at progressively longer times, the amount of β-phase increases faster than that of α-phase.

An example of the evolution of the α- and β-peak melting enthalpies during crystallization of QQ containing PP droplets is shown in Fig. 17b and c, respectively, together with the corresponding Avrami fittings. Also, in this case, an Avrami exponent close to one is obtained, thus confirming that β-nucleated PP droplets crystallize according to a nucleation-controlled regime, analogously to the previously discussed heterogeneously nucleated droplet systems. From the trend of the melting endotherms and of the melting enthalpies, it must be deduced that, since QQ possesses a dual nucleating ability, nucleation of either α- or β-crystals occur in each droplet, according to the nucleating agent selectivity at the chosen crystallization temperature. Thus, some droplets will contain exclusively α- and some others β-form, with the possibility of β-phase nucleating on top of α-phase crystals (known as growth transition or cross-nucleation [95,96]) being disregarded due to the limited droplet size and extremely short polymorph growth time.

Now that the capability of studying droplets in immiscible blends nucleated by a variety of additives has been assessed, the directly measured heterogeneous nucleation rate can be used to derive an "intrinsic" nucleation efficiency scale. To this aim, the heterogeneous nucleation model of a polymer onto a substrate described in Section 2.2 (equation (5)) can be applied.

Fig. 18a summarizes the nucleation rate data for the various α- and β-nucleated droplets, plotted according to equation (5), and including the data for neat PS/PP blend for the sake of comparison. As described in Section 2.2, the parameter $\Delta\sigma$ can be obtained from the slope of the line that fits the data. Thus, the slope of the plots in Fig. 18a is directly proportional to the free energy barrier for nucleation. The isothermal crystallization kinetics of the neat blend, which occurs onto unknown impurities or at the interface with PS, can be considered a less efficient α-form nucleating agent. Therefore, for the α-phase, the slope increases in the order NA-11 < sodium benzoate < unknown impurities/PS surface. In the case of the β-crystals, the temperature dependence of the nucleation rate data according to equation (5) is much steeper for QQ than for DCHT.

The derived values of $\Delta\sigma$ for the various substrates and the two polymorphs are reported in Fig. 18b. As discussed in Section 2.2, the lower the interfacial free energy difference, the highest the nucleating efficiency of the given substrate. The $\Delta\sigma$ of the α-phase nucleating agents obtained by the droplet technique can be compared with similar values reported in the literature. A wealth of data on heterogeneous nucleation rates can be found in the literature concerning fiber-induced crystallization of PP [97,98]. The best nucleating fiber, i.e., poly(tetrafluoroethylene) has a $\Delta\sigma$ of about 5 mJ/m^2, which is slightly higher than those shown in Fig. 18b for sodium benzoate and NA-11. Different values of interfacial free energy difference have been found for these two nucleating agents by using different measurement methods or different heterogeneous nucleation models [69,99]. However, the discrepancy between the values derived from the nucleated droplet technique and those in the literature is within a reasonable 15% [17].

For the β-phase, the free energy barrier for nucleation on QQ is about double the one for nucleating onto DCHT. Moreover, the DCHT $\Delta\sigma$ value below unity is likely due to the known occurrence of epitaxial nucleation [92], as previously discussed in Section 2.2 for the case of HDPE/PP surface nucleation. For QQ, no epitaxial crystallization with β-PP is

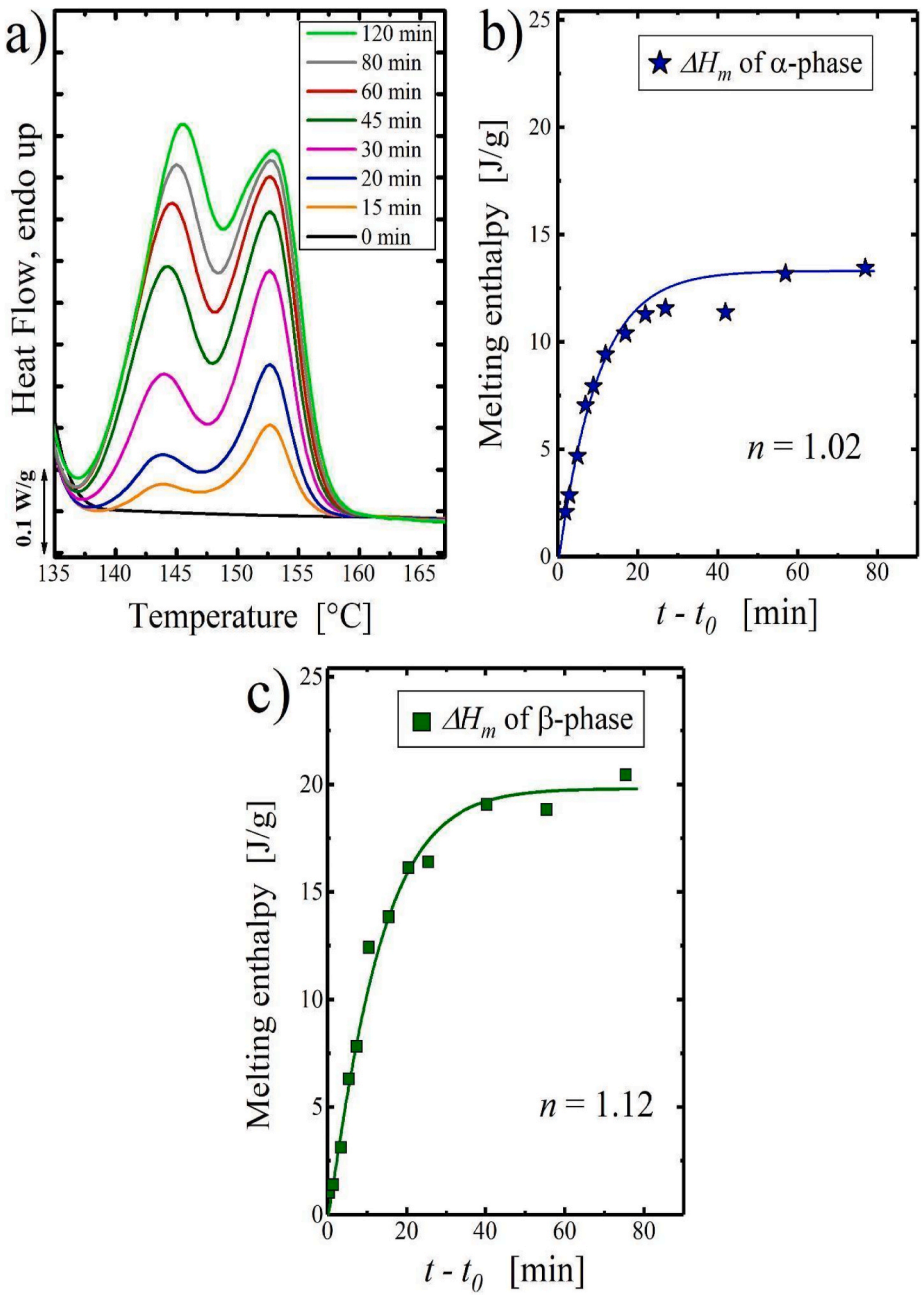

Fig. 17. (a) DSC final heating scans of the 80/20/2 wt%/wt%/wt% PS/PP/QQ blend after isothermal crystallization at 131 °C for different times. (b, c) present the evolution of the melting enthalpy of the α-phase and β-phase, respectively, in the 80/20/2 wt %/wt%/wt% PS/PP/QQ blend, calculated from the heating scans after isothermal crystallization at 128 °C for different times. Solid lines in (b,c) are the fitting of (b) α-phase and (c) β-phase data using the Avrami equation (1); the calculated Avrami indexes (*n*) are also reported.[91]Adapted with permission from the Royal Society of Chemistry.

reported, although it is confirmed for the structurally similar γ-quinacridone [100]. Thus, the higher interfacial free energy difference with respect to DCHT might be due to a worse crystallographic matching between PP and QQ in comparison to that between PP and DCHT.

The work presented in this Section demonstrates the possibility of heterogeneously nucleate droplets in immiscible blends and shows how this strategy can be used to derive fundamental information on nucleating agents and the heterogeneous nucleation process in general.

3. Conclusions and outlook

In this Feature Article, we described in detail the major nucleation modalities of semicrystalline droplets dispersed in an immiscible blend, based on our recent works in the topic [3,17,74,79,91]. Immiscible blends with droplet-in-matrix morphology are an interesting system for learning about several nucleation aspects. In fact, when the number of droplets is high enough, they are statistically clean of nucleating impurities, and different effects can be highlighted.

These clean droplets usually crystallize at large undercooling, but their solidification behaviour can be drastically changed by injecting self-nuclei into them. Self-nucleation provokes an increase in the droplet population crystallizing at high temperatures, comparable to the ones of the self-nucleated bulk polymer. Moreover, if the self-nucleation conditions are ideal, i.e., for T_S at the lower limit of *Domain II*, the free energy barrier for primary nucleation becomes negligible. Thus, in such conditions, the overall crystallization is dominated by crystal growth, contrary to that of droplets self-nucleated in *Domain I*, notwithstanding the small droplet volume.

Clean droplets which are not self-nucleated commonly nucleate at the interface with the immiscible matrix since the nucleation barrier for homogeneous nucleation is typically higher than that of surface-induced nucleation. For blends made by two semicrystalline polymers, the occurrence of surface nucleation can be demonstrated by showing the correlation between droplet and matrix overall crystallization kinetics

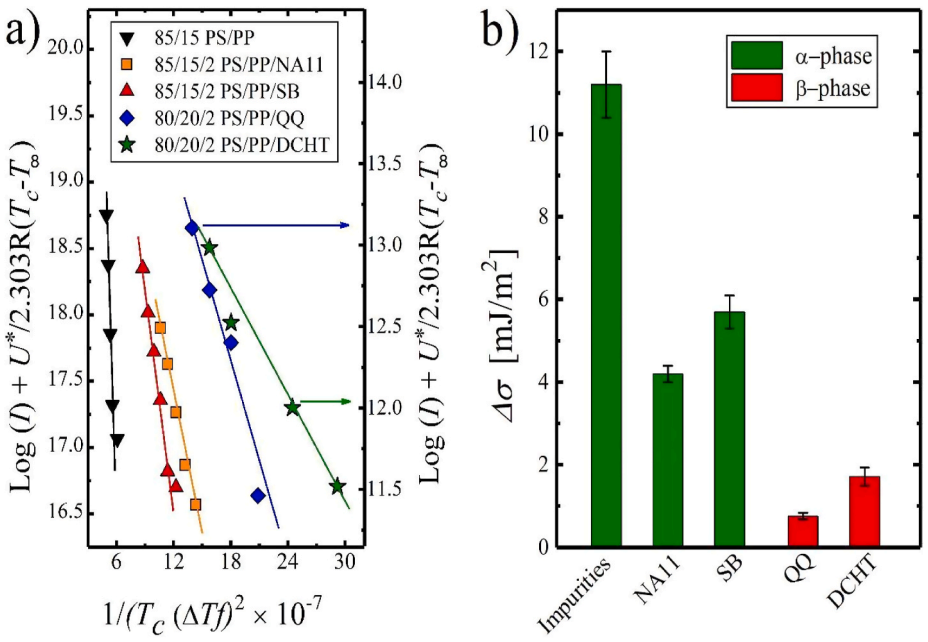

Fig. 18. (a) Temperature dependence of the nucleation rate of PP droplets in the indicated systems according to equation (5). (b) Calculated $\Delta\sigma$ value for α- and β-phase of PP with different heterogeneous nucleating agents or substrates.

when the latter is changed via a self-nucleation protocol. By applying this method with different polymer pairs, we demonstrated that surface nucleation is most efficient for polymers for which an epitaxial nucleation mechanism is active at the interface.

Besides the above-mentioned crystallographic interactions, the interfacial surface roughness can also play a major role in droplet nucleation. In particular, it is shown that the self-nucleation temperature range (i.e., *Domain II* and specifically, *Domain IIa*) of HDPE in immiscible blends can be greatly enlarged, up to temperatures above its equilibrium melting temperature, with respect to the same polymer in bulk. Morphological evidences indicate that this is due to the formation of a rough interface between the two polymers during heating to T_S (for amorphous matrices with relatively low T_g), or during crystallization of the matrix at high temperatures (for a semicrystalline major component), which provides abundant surface nucleation sites on recrystallization.

Eventually, impurity-free droplets can conveniently be used to scout the intrinsic nucleating efficiency of nucleating agents. If nucleating additives are added to the droplet systems, they provide heterogeneous seeds for nucleation and increase the droplet population that crystallizes at lower undercoolings. Moreover, analogously to clean dropets, the overall crystallization kinetics of such heterogeneously nucleated droplets displays a first-order kinetics, the signature of a nucleation-controlled crystallization mechanism. Therefore, this strategy gives direct access to heterogeneous nucleation rate measurements and enables the application of nucleation rate models that provide the free energy barrier of the process, on the base of which different nucleating additives can be meaningfully compared.

In order to understand whether the crystallization kinetics of a droplet ensemble is truly governed by nucleation, and the contribution of crystal growth can be safely neglected, we have introduced the use of a dimensionless parameter named the "Turnbull number". This number is given by the ratio of the time required to grow a crystal inside the average droplet volume divided by the time needed for nucleation to occur in the same droplet. Therefore, Turnbull numbers close to unity indicate that the droplet crystallization is dominated by crystal growth, as in the case of self-nucleated droplets or of HDPE droplets crystallized at relatively large undercoolings. In these cases, sigmoidal overall crystallization kinetics (second or third order) is also found. Instead, droplets for which the crystallization is controlled by nucleation have Turnbull numbers typically lower than 0.1–0.01 and display a first-order crystallization kinetics.

This Feature Article did not explore in detail the case of homogeneous nucleation, as it is not very common in immiscible blends due to the typically prevailing surface nucleation mechanism. However, if a sufficiently inert substrate would be found for a given system, a study of homogenous nucleation in polymer blends, including the role of droplet phase sizes on nucleation rate, would be highly interesting. For what concerns the topic of surface nucleation, compelling proofs of its occurrence have been reported in the case of double semicrystalline polymer blends with droplet morphology. On the other hand, the case of amorphous matrices still needs to be explored in detail, particularly bringing evidence of surface nucleation and a further understanding of the mechanism, being any crystallographic matching impossible. Heterogeneously nucleated droplets can be further studied to improve our fundamental knowledge of nucleating agents. If this topic is pursued, a better description of the migration of nucleating impurities between matrix and droplet phases could be achieved.

Funding

All of the sources of funding for the work described in this publication are acknowledged below:

This work has received funding from the Basque Government through grant IT1503-22. We would also like to acknowledge the financial support from the BIODEST and the REPOL projects; these projects have received funding from the European Union's Horizon 2020 research and innovation program under the Marie Skłodowska-Curie grant agreements No. 778092and No. 860221.

Declaration of competing interest

The authors declare that they have no known competing financial interests or personal relationships that could have appeared to influence the work reported in this paper.

Data availability

Data will be made available on request.

Acknowledgements

The experimental work of Bao Wang, Enrico Carmeli, Sara Ottonello, Wei Wang, and Simona Buzzi is acknowledged. This work has received funding from the Basque Government through grant IT1503-22. We would also like to acknowledge the financial support from the BIODEST and the REPOL projects; these projects have received funding from the European Union's Horizon 2020 research and innovation program under the Marie Skłodowska-Curie grant agreements No. 778092 and No. 860221.

References

[1] H. Frensch, P. Harnischfeger, B.-J. Jungnickel, Fractionated crystallization in incompatible polymer blends, in: Multiphase Polymers: Blends and Ionomers; ACS Symposium Series, 395, American Chemical Society, 1989, pp. 101–125, https://doi.org/10.1021/bk-1989-0395.ch005.

[2] M.L. Arnal, M.E. Matos, R.A. Morales, O.O. Santana, A.J. Müuller, Evaluation of the fractionated crystallization of dispersed polyolefins in a polystyrene matrix, Macromol. Chem. Phys. 199 (10) (1998) 2275–2288, https://doi.org/10.1002/(SICI)1521-3935(19981001)199:10<2275::AID-MACP2275>3.0.CO;2-#.

[3] L. Sangroniz, B. Wang, Y. Su, G. Liu, D. Cavallo, D. Wang, A.J. Müller, Fractionated crystallization in semicrystalline polymers, Prog. Polym. Sci. 115 (2021), 101376, https://doi.org/10.1016/j.progpolymsci.2021.101376.

[4] J.L. Carvalho, K. Dalnoki-Veress, Homogeneous bulk, surface, and edge nucleation in crystalline nanodroplets, Phys. Rev. Lett. 105 (23) (2010), 237801, https://doi.org/10.1103/PhysRevLett.105.237801.

[5] U.W. Gedde, M.S. Hedenqvist, Fundamental Polymer Science, Graduate texts in physics, second ed., Springer, Cham, Switzerland, 2019.

[6] D. Cavallo, A.J. Müller, Polymer crystallization, in: N. Hadjichristidis, Y. Gnanou, K. Matyjaszewski, M. Muthukumar (Eds.), Macromolecular Engineering, Wiley, 2022, pp. 1–57, https://doi.org/10.1002/9783527815562.mme0032.

[7] M. Avrami, Kinetics of phase change. I general theory, J. Chem. Phys. 7 (12) (1939) 1103–1112, https://doi.org/10.1063/1.1750380.

[8] M. Avrami, Kinetics of phase change. II transformation-time relations for random distribution of nuclei, J. Chem. Phys. 8 (2) (1940) 212–224, https://doi.org/10.1063/1.1750631.

[9] M. Granulation Avrami, Phase change, and microstructure kinetics of phase change. III, J. Chem. Phys. 9 (2) (1941) 177–184, https://doi.org/10.1063/1.1750872.

[10] M. Fanfoni, M. Tomellini, The johnson-mehl- avrami-kohnogorov model: a brief review, Il Nuovo Cimento D 20 (7) (1998) 1171–1182, https://doi.org/10.1007/BF03185527.

[11] A.T. Lorenzo, M.L. Arnal, J. Albuerne, A.J. Müller, DSC isothermal polymer crystallization kinetics measurements and the use of the Avrami equation to fit the data: guidelines to avoid common problems, Polym. Test. 26 (2) (2007) 222–231, https://doi.org/10.1016/j.polymertesting.2006.10.005.

[12] E. Piorkowska, A. Galeski, J.-M. Haudin, Critical assessment of overall crystallization kinetics theories and predictions, Prog. Polym. Sci. 31 (6) (2006) 549–575, https://doi.org/10.1016/j.progpolymsci.2006.05.001.

[13] R.A. Pérez-Camargo, G.-M. Liu, D.-J. Wang, A.J. Müller, Experimental and data fitting guidelines for the determination of polymer crystallization kinetics, Chin. J. Polym. Sci. 40 (6) (2022) 658–691, https://doi.org/10.1007/s10118-022-2724-2.

[14] V. Balsamo, N. Urdaneta, L. Pérez, P. Carrizales, V. Abetz, A.J. Müller, Effect of the polyethylene confinement and topology on its crystallisation within semicrystalline ABC triblock copolymers, Eur. Polym. J. 40 (6) (2004) 1033–1049, https://doi.org/10.1016/j.eurpolymj.2004.01.009.

[15] A.J. Müller, V. Balsamo, M.L. Arnal, Nucleation and crystallization in diblock and triblock copolymers, in: V. Abetz (Ed.), Block Copolymers II, Springer Berlin Heidelberg, Berlin, Heidelberg, 2005, pp. 1–63, https://doi.org/10.1007/12_001.

[16] M.E. Córdova, A.T. Lorenzo, A.J. Müller, L. Gani, S. Tencé-Girault, L. Leibler, The influence of blend morphology (Co-continuous or sub-micrometer droplets dispersions) on the nucleation and crystallization kinetics of double crystalline polyethylene/polyamide blends prepared by reactive extrusion: the influence of blend morphology (Co-continuous or sub-micrometer droplets dispersions), Macromol. Chem. Phys. 212 (13) (2011) 1335–1350, https://doi.org/10.1002/macp.201100039.

[17] B. Wang, R. Utzeri, M. Castellano, P. Stagnaro, A.J. Müller, D. Cavallo, Heterogeneous nucleation and self-nucleation of isotactic polypropylene microdroplets in immiscible blends: from nucleation to growth-dominated crystallization, Macromolecules 53 (14) (2020) 5980–5991, https://doi.org/10.1021/acs.macromol.0c01167.

[18] R.L. Cormia, F.P. Price, D. Turnbull, Kinetics of crystal nucleation in polyethylene, J. Chem. Phys. 37 (6) (1962) 1333–1340, https://doi.org/10.1063/1.1733282.

[19] J.R. Burns, D. Turnbull, Kinetics of crystal nucleation in molten isotactic polypropylene, J. Appl. Phys. 37 (11) (1966) 4021–4026, https://doi.org/10.1063/1.1707969.

[20] J.A. Koutsky, A.G. Walton, E. Baer, Nucleation of polymer droplets, J. Appl. Phys. 38 (4) (1967) 1832–1839, https://doi.org/10.1063/1.1709769.

[21] R.M. Michell, I. Blaszczyk-Lezak, C. Mijangos, A.J. Müller, Confinement effects on polymer crystallization: from droplets to alumina nanopores, Polymer 54 (16) (2013) 4059–4077, https://doi.org/10.1016/j.polymer.2013.05.029.

[22] R.T. Tol, V.B.F. Mathot, G. Groeninckx, Confined crystallization phenomena in immiscible polymer blends with dispersed micro – and nanometer sized PA6 droplets, Part 1: uncompatibilized PS/PA6, (PPE/PS)/PA6 and PPE/PA6 blends, Polymer 46 (2) (2005) 369–382, https://doi.org/10.1016/j.polymer.2004.10.085.

[23] R.T. Tol, V.B.F. Mathot, G. Groeninckx, Confined crystallization phenomena in immiscible polymer blends with dispersed micro- and nanometer sized PA6 droplets, Part 2: reactively compatibilized PS/PA6 and (PPE/PS)/PA6 blends, Polymer 46 (2) (2005) 383–396, https://doi.org/10.1016/j.polymer.2004.10.070.

[24] R.T. Tol, V.B.F. Mathot, G. Groeninckx, Confined crystallization phenomena in immiscible polymer blends with dispersed micro- and nanometer sized PA6 droplets, Part 3: crystallization kinetics and crystallinity of micro- and nanometer sized PA6 droplets crystallizing at high supercoolings, Polymer 46 (9) (2005) 2955–2965, https://doi.org/10.1016/j.polymer.2005.02.020.

[25] M.S. Sánchez, V. Mathot, G.V. Poel, G. Groeninckx, W. Bruls, Crystallization of polyamide confined in sub-micrometer droplets dispersed in a molten polyethylene matrix, J. Polym. Sci., Part B: Polym. Phys. 44 (5) (2006) 815–825, https://doi.org/10.1002/polb.20738.

[26] T.E. Bernal-Lara, R.Y.F. Liu, A. Hiltner, E. Baer, Structure and thermal stability of polyethylene nanolayers, Polymer 46 (9) (2005) 3043–3055, https://doi.org/10.1016/j.polymer.2005.01.055.

[27] Y. Jin, A. Hiltner, E. Baer, Fractionated crystallization of polypropylene droplets produced by nanolayer breakup, J. Polym. Sci., Part B: Polym. Phys. 45 (10) (2007) 1138–1151, https://doi.org/10.1002/polb.21146.

[28] R.M. Michell, A.J. Müller, Confined crystallization of polymeric materials, Prog. Polym. Sci. 54 (55) (2016) 183–213, https://doi.org/10.1016/j.progpolymsci.2015.10.007.

[29] A.J. Müller, V. Balsamo, M.L. Arnal, T. Jakob, H. Schmalz, V. Abetz, Homogeneous nucleation and fractionated crystallization in block copolymers, Macromolecules 35 (8) (2002) 3048–3058, https://doi.org/10.1021/ma012026w.

[30] R.V. Castillo, A.J. Müller, Crystallization and morphology of biodegradable or biostable single and double crystalline block copolymers, Prog. Polym. Sci. 34 (6) (2009) 516–560, https://doi.org/10.1016/j.progpolymsci.2009.03.002.

[31] S. Nakagawa, H. Marubayashi, S. Nojima, Crystallization of polymer chains confined in nanodomains, Eur. Polym. J. 70 (2015) 262–275, https://doi.org/10.1016/j.eurpolymj.2015.07.018.

[32] R.M. Michell, I. Blaszczyk-Lezak, C. Mijangos, A.J. Müller, Confined crystallization of polymers within anodic aluminum oxide templates, J. Polym. Sci., Part B: Polym. Phys. 52 (18) (2014) 1179–1194, https://doi.org/10.1002/polb.23553.

[33] G. Liu, A.J. Müller, D. Wang, Confined crystallization of polymers within nanopores, Acc. Chem. Res. 54 (15) (2021) 3028–3038, https://doi.org/10.1021/acs.accounts.1c00242.

[34] D.J. Blundell, A. Keller, A.J. Kovacs, A new self-nucleation phenomenon and its application to the growing of polymer crystals from solution, J. Polym. Sci. [B] 4 (7) (1966) 481–486, https://doi.org/10.1002/pol.1966.110040709.

[35] B. Fillon, J.C. Wittmann, B. Lotz, A. Thierry, Self-nucleation and recrystallization of isotactic polypropylene (α phase) investigated by differential scanning Calorimetry, J. Polym. Sci., Part B: Polym. Phys. 31 (10) (1993) 1383–1393, https://doi.org/10.1002/polb.1993.090311013.

[36] R.M. Michell, A. Mugica, M. Zubitur, A.J. Müller, Self-nucleation of crystalline phases within homopolymers, polymer blends, copolymers, and nanocomposites, in: F. Auriemma, G.C. Alfonso, C. de Rosa (Eds.), Polymer Crystallization I: from Chain Microstructure to Processing, Springer International Publishing, Cham, 2017, pp. 215–256, https://doi.org/10.1007/12_2015_327.

[37] L. Sangroniz, D. Cavallo, A. Müller, J. Self-nucleation effects on polymer crystallization, Macromolecules 53 (12) (2020) 4581–4604, https://doi.org/10.1021/acs.macromol.0c00223.

[38] L. Sangroniz, D. Cavallo, A. Santamaria, A.J. Müller, R.G. Alamo, Thermorheologically complex self-seeded melts of propylene–ethylene copolymers, Macromolecules 50 (2) (2017) 642–651, https://doi.org/10.1021/acs.macromol.6b02392.

[39] L. Sangroniz, F. Barbieri, D. Cavallo, A. Santamaria, R.G. Alamo, A. Müller, J. Rheology of self-nucleated poly(ϵ-caprolactone) melts, Eur. Polym. J. 99 (2018) 495–503, https://doi.org/10.1016/j.eurpolymj.2018.01.009.

[40] L. Sangroniz, R.G. Alamo, D. Cavallo, A. Santamaría, A.J. Müller, A. Alegría, Differences between isotropic and self-nucleated PCL melts detected by dielectric experiments, Macromolecules 51 (10) (2018) 3663–3671, https://doi.org/10.1021/acs.macromol.8b00708.

[41] L. Sangroniz, A. Sangroniz, L. Meabe, A. Basterretxea, H. Sardon, D. Cavallo, A. J. Müller, Chemical structure drives memory effects in the crystallization of homopolymers, Macromolecules 53 (12) (2020) 4874–4881, https://doi.org/10.1021/acs.macromol.0c00751.

[42] L. Sangroniz, Y.-J. Jang, M.A. Hillmyer, A.J. Müller, The role of intermolecular interactions on melt memory and thermal fractionation of semicrystalline

polymers, J. Chem. Phys. 156 (14) (2022), 144902, https://doi.org/10.1063/5.0087782.
[43] R.A. Morales, M.L. Arnal, A.J. Müller, The evaluation of the state of dispersion in immiscible blends where the minor phase exhibits fractionated crystallization, Polym. Bull. 35 (3) (1995) 379–386, https://doi.org/10.1007/BF00963138.
[44] A.C. Manaure, A.J. Müller, Nucleation and crystallization of blends of poly (propylene) and ethylene/α-olefin copolymers, Macromol. Chem. Phys. 201 (9) (2000) 958–972, https://doi.org/10.1002/1521-3935(20000601)201:9<958::AID-MACP958>3.0.CO;2-0.
[45] J.I. Lauritzen, J.D. Hoffman, formation of polymer crystals with folded chains from dilute solution, J. Chem. Phys. 31 (6) (1959) 1680–1681, https://doi.org/10.1063/1.1730678.
[46] J.D. Hoffman, R.L. Miller, Kinetic of crystallization from the melt and chain folding in polyethylene fractions revisited: theory and experiment, Polymer 38 (13) (1997) 3151–3212, https://doi.org/10.1016/S0032-3861(97)00071-2.
[47] W.S. Lambert, P.J. Phillips, Crystallization kinetics of low molecular weight fractions of branched polyethylenes, Macromolecules 27 (13) (1994) 3537–3542, https://doi.org/10.1021/ma00091a014.
[48] S. Andjelić, D. Jamiolkowski, J. McDivitt, J. Fischer, J. Zhou, R. Vetrecin, Crystallization study on absorbable poly(p-dioxanone) polymers by differential scanning Calorimetry, J. Appl. Polym. Sci. 79 (4) (2001) 742–759, https://doi.org/10.1002/1097-4628(20010124)79:4<742::AID-APP190>3.0.CO;2-J.
[49] A.J. Müller, J. Albuerne, L. Marquez, J.-M. Raquez, P. Degée, P. Dubois, J. Hobbs, I.W. Hamley, Self-nucleation and crystallization kinetics of double crystalline poly(p-dioxanone)-b-poly(ε-caprolactone) diblock copolymers, 0, Faraday Discuss 128 (2005) 231–252, https://doi.org/10.1039/B403085K.
[50] A.T. Lorenzo, M.L. Arnal, A.J. Müller, A. Boschetti-de-Fierro, V. Abetz, Nucleation and isothermal crystallization of the polyethylene block within diblock copolymers containing polystyrene and poly(ethylene-alt-propylene), Macromolecules 40 (14) (2007) 5023–5037, https://doi.org/10.1021/ma070252l.
[51] A.T. Lorenzo, A.J. Müller, Estimation of the nucleation and crystal growth contributions to the overall crystallization energy barrier, J. Polym. Sci., Part B: Polym. Phys. 46 (14) (2008) 1478–1487, https://doi.org/10.1002/polb.21483.
[52] P.J. Barham, D.A. Jarvis, A. Keller, A new look at the crystallization of polyethylene. III. Crystallization from the melt at high supercoolings, J. Polym. Sci. Polym. Phys. Ed 20 (9) (1982) 1733–1748, https://doi.org/10.1002/pol.1982.180200922.
[53] M.V. Massa, K. Dalnoki-Veress, Homogeneous crystallization of poly(ethylene oxide) confined to droplets: the dependence of the crystal nucleation rate on length scale and temperature, Phys. Rev. Lett. 92 (25) (2004), 255509, https://doi.org/10.1103/PhysRevLett.92.255509.
[54] D.S. Langhe, A. Hiltner, E. Baer, Effect of additives, catalyst residues, and confining substrates on the fractionated crystallization of polypropylene droplets, J. Appl. Polym. Sci. 125 (3) (2012) 2110–2120, https://doi.org/10.1002/app.36300.
[55] O.T. Ikkala, R.M. Holsti-Miettinen, J. Seppälä, Effects of compatibilization on fractionated crystallization of PA6/PP blends, J. Appl. Polym. Sci. 49 (7) (1993) 1165–1174, https://doi.org/10.1002/app.1993.070490705.
[56] E. Carmeli, S.E. Fenni, M.R. Caputo, A.J. Müller, D. Tranchida, D. Cavallo, Surface nucleation of dispersed polyethylene droplets in immiscible blends revealed by polypropylene matrix self-nucleation, Macromolecules 54 (19) (2021) 9100–9112, https://doi.org/10.1021/acs.macromol.1c01430.
[57] B. Lotz, J.C. Wittmann, Structural relationships in blends of isotactic polypropylene and polymers with aliphatic sequences, J. Polym. Sci., Part B: Polym. Phys. 24 (7) (1986) 1559–1575, https://doi.org/10.1002/polb.1986.090240713.
[58] B. Lotz, J.C. Wittmann, Polyethylene–isotactic polypropylene epitaxy: analysis of the diffraction patterns of oriented biphasic blends, J. Polym. Sci., Part B: Polym. Phys. 25 (5) (1987) 1079–1087, https://doi.org/10.1002/polb.1987.090250509.
[59] A.J. Greso, P.J. Phillips, The role of secondary nucleation in epitaxial growth: the template model, Polymer 35 (16) (1994) 3373–3376, https://doi.org/10.1016/0032-3861(94)90897-4.
[60] S. Yan, J. Petermann, D. Yang, Effect of lamellar thickness on the epitaxial crystallization of PE on oriented IPP films, Polym. Bull. 38 (1) (1997) 87–94, https://doi.org/10.1007/s002890050023.
[61] S. Yan, D. Yang, J. Petermann, Controlling factors for the occurrence of heteroepitaxy of polyethylene on highly oriented isotactic polypropylene, Polymer 39 (19) (1998) 4569–4578, https://doi.org/10.1016/S0032-3861(97)10137-9.
[62] B. Fillon, B. Lotz, A. Thierry, J.C. Wittmann, Self-nucleation and enhanced nucleation of polymers. Definition of a convenient calorimetric “efficiency scale” and evaluation of nucleating additives in isotactic polypropylene (α phase), J. Polym. Sci., Part B: Polym. Phys. 31 (10) (1993) 1395–1405, https://doi.org/10.1002/polb.1993.090311014.
[63] M. Trujillo, M.L. Arnal, A.J. Müller, E. Laredo, St Bredeau, D. Bonduel, Ph Dubois, Thermal and morphological characterization of nanocomposites prepared by in-situ polymerization of high-density polyethylene on carbon nanotubes, Macromolecules 40 (17) (2007) 6268–6276, https://doi.org/10.1021/ma071025m.
[64] A.J. Müller, M.L. Arnal, M. Trujillo, A.T. Lorenzo, Super-nucleation in nanocomposites and confinement effects on the crystallizable components within block copolymers, miktoarm star copolymers and nanocomposites, Des. Polym. Control. Synth. Struct.-Prop. Relatsh. Appl. Dedic. Profr. Nikos Hadjichristidis Recognit. His Contrib. Polym. Sci. 47 (4) (2011) 614–629, https://doi.org/10.1016/j.eurpolymj.2010.09.027.
[65] M. Trujillo, M.L. Arnal, A.J. Müller, M.A. Mujica, C. Urbina de Navarro, B. Ruelle, P. Dubois, Supernucleation and crystallization regime change provoked by MWNT addition to poly(ε-caprolactone), Polymer 53 (3) (2012) 832–841, https://doi.org/10.1016/j.polymer.2011.12.028.
[66] M.J. Galante, L. Mandelkern, R.G. Alamo, A. Lehtinen, R. Paukker, Crystallization kinetics of metallocene type polypropylenes, J. Therm. Anal. 47 (4) (1996) 913–929, https://doi.org/10.1007/BF01979439.
[67] B. Wunderlich, Chapter V - the nucleation step, in: Macromolecular Physics, 2, Academic Press, 1976, 1–114.
[68] F. Price, in: Nucleation, A. Zettlemoyer (Eds.), Nucleation in Polymer Crystallization, 1969. New York.
[69] E. Carmeli, B. Wang, P. Moretti, D. Tranchida, D. Cavallo, Estimating the nucleation ability of various surfaces towards isotactic polypropylene via light intensity induction time measurements, Entropy 21 (11) (2019), https://doi.org/10.3390/e21111068.
[70] H. Ishida, P. Bussi, Surface induced crystallization in ultrahigh-modulus polyethylene fiber-reinforced polyethylene composites, Macromolecules 24 (12) (1991) 3569–3577, https://doi.org/10.1021/ma00012a017.
[71] H. Ishida, P. Bussi, Induction time approach to surface induced crystallization in polyethylene/poly (ε-Caprolactone) melt, J. Mater. Sci. 26 (23) (1991) 6373–6382, https://doi.org/10.1007/BF02387817.
[72] W. Wang, B. Wang, A. Tercjak, A.J. Müller, Z. Ma, D. Cavallo, Origin of transcrystallinity and nucleation kinetics in polybutene-1/fiber composites, Macromolecules 53 (20) (2020) 8940–8950, https://doi.org/10.1021/acs.macromol.0c02038.
[73] S. Coba-Daza, E. Carmeli, I. Otaegi, N. Aranburu, G. Guerrica-Echevarria, S. Kahlen, D. Cavallo, D. Tranchida, A.J. Müller, Effect of Compatibilizer Addition on the Surface Nucleation of Dispersed Polyethylene Droplets in a Self-Nucleated Polypropylene Matrix, Polymer 263 (2022) 125511, https://doi.org/10.1016/j.polymer.2022.125511.
[74] W. Wang, S. Buzzi, S.E. Fenni, E. Carmeli, B. Wang, G. Liu, A.J. Müller, D. Cavallo, Surface Nucleation of Dispersed Droplets in Double Semicrystalline Immiscible Blends with Different Matrices, Macromol. Chem. Phys. (2022) 2200202, https://doi.org/10.1002/macp.202200202.
[75] C. Yan, H. Li, J. Zhang, Y. Ozaki, D. Shen, D. Yan, A.-C. Shi, S. Yan, Surface-induced anisotropic chain ordering of polycarprolactone on oriented polyethylene substrate: epitaxy and soft epitaxy, Macromolecules 39 (23) (2006) 8041–8048, https://doi.org/10.1021/ma061188v.
[76] H. Chang, J. Zhang, L. Li, Z. Wang, C. Yang, I. Takahashi, Y. Ozaki, S. Yan, A study on the epitaxial ordering process of the polycaprolactone on the highly oriented polyethylene substrate, Macromolecules 43 (1) (2010) 362–366, https://doi.org/10.1021/ma902235f.
[77] J. Hu, R. Xin, C.-Y. Hou, S.-K. Yan, J.-C. Liu, Direct comparison of crystal nucleation activity of PCL on patterned substrates, Chin. J. Polym. Sci. 37 (7) (2019) 693–699, https://doi.org/10.1007/s10118-019-2226-z.
[78] W. Wang, B. Wang, E. Carmeli, Z. Wang, Z. Ma, D. Cavallo, Cross-nucleation of polybutene-1 form II on form I seeds with different morphology, Polym. Cryst. 3 (2) (2020), e210104, https://doi.org/10.1002/pcr2.10104.
[79] S.E. Fenni, M.R. Caputo, A.J. Müller, D. Cavallo, Surface roughness enhances self-nucleation of high-density polyethylene droplets dispersed within immiscible blends, Macromolecules 55 (4) (2022) 1412–1423, https://doi.org/10.1021/acs.macromol.1c02487.
[80] Z. Bartczak, A. Gałeski, Changes in interface shape during crystallization in two-component polymer systems, Polymer 27 (4) (1986) 544–548, https://doi.org/10.1016/0032-3861(86)90240-5.
[81] J.A. Koutsky, A.G. Walton, E. Baer, Heterrogeneous nucleation of polyethylene melts on cleaved surfaces of alkali halides, J. Polym. Sci. [B] 5 (2) (1967) 185–190, https://doi.org/10.1002/pol.1967.110050210.
[82] J.L. Carvalho, K. Dalnoki-Veress, Surface nucleation in the crystallisation of polyethylene droplets, Eur. Phys. J. E 34 (1) (2011) 6, https://doi.org/10.1140/epje/i2011-11006-y.
[83] M. Tariq, T. Thurn-Albrecht, O. Dolynchuk, Heterogeneous crystal nucleation from the melt in polyethylene oxide droplets on graphite: kinetics and microscopic structure, Crystals 11 (8) (2021), https://doi.org/10.3390/cryst11080924.
[84] M.K. Hoffmeyer, J.H. Perepezko, Nucleation catalysis by dispersed particles, Scripta Metall. 22 (7) (1988) 1143–1148, https://doi.org/10.1016/S0036-9748(88)80120-0.
[85] O.O. Santana, A.J. Müller, Homogeneous nucleation of the dispersed crystallisable component of immiscible polymer blends, Polym. Bull. 32 (4) (1994) 471–477, https://doi.org/10.1007/BF00587890.
[86] Y. Jin, A. Hiltner, E. Baer, Effect of a sorbitol nucleating agent on fractionated crystallization of polypropylene droplets, J. Polym. Sci., Part B: Polym. Phys. 45 (14) (2007) 1788–1797, https://doi.org/10.1002/polb.21195.
[87] Y. Jin, A. Hiltner, E. Baer, Effect of an organic dicarboxylic acid salt on fractionated crystallization of polypropylene droplets, J. Appl. Polym. Sci. 105 (6) (2007) 3260–3273, https://doi.org/10.1002/app.26584.
[88] D.S. Langhe, J.K. Keum, A. Hiltner, E. Baer, Fractionated crystallization of α- and β-nucleated polypropylene droplets, J. Polym. Sci., Part B: Polym. Phys. 49 (2) (2011) 159–171, https://doi.org/10.1002/polb.22162.
[89] Z. Bartczak, A. Galeski, N.P. Krasnikova, Primary nucleation and spherulite growth rate in isotactic polypropylene-polystyrene blends, Polymer 28 (10) (1987) 1627–1634, https://doi.org/10.1016/0032-3861(87)90002-4.
[90] D. Kashchiev, D. Clausse, C. Jolivet-Dalmazzone, Crystallization and critical supercooling of disperse liquids, J. Colloid Interface Sci. 165 (1) (1994) 148–153, https://doi.org/10.1006/jcis.1994.1215.

[91] E. Carmeli, S. Ottonello, B. Wang, A. Menyhárd, A.J. Müller, D. Cavallo, Competing crystallization of α- and β-phase induced by β-nucleating agents in microdroplets of isotactic polypropylene, CrystEngComm 24 (10) (2022) 1966–1978, https://doi.org/10.1039/D2CE00087C.
[92] Z. Wang, W. Yang, G. Liu, A.J. Müller, Y. Zhao, X. Dong, K. Wang, D. Wang, Probing into the epitaxial crystallization of β form isotactic polypropylene: from experimental observations to molecular mechanics computation, J. Polym. Sci., Part B: Polym. Phys. 55 (5) (2017) 418–424, https://doi.org/10.1002/polb.24293.
[93] C. Mathieu, A. Thierry, J.C. Wittmann, B. Lotz, Specificity and versatility of nucleating agents toward isotactic polypropylene crystal phases, J. Polym. Sci., Part B: Polym. Phys. 40 (22) (2002) 2504–2515, https://doi.org/10.1002/polb.10309.
[94] J. Varga, K. Stoll, A. Menyhárd, Z. Horváth, Crystallization of isotactic polypropylene in the presence of a β-nucleating agent based on a trisamide of trimesic acid, J. Appl. Polym. Sci. 121 (3) (2011) 1469–1480, https://doi.org/10.1002/app.33685.
[95] J. Varga, A. Ille, Y. Fujiwara, Bα-bifurcation of growth during the spherulitic crystallization of polypropylene, Period. Polytech. - Chem. Eng. 34 (4) (1990) 255–271.
[96] S. Looijmans, A. Menyhard, G.W.M. Peters, G.C. Alfonso, D. Cavallo, Anomalous temperature dependence of isotactic polypropylene α-on-β cross-nucleation kinetics, Cryst. Growth Des. 17 (9) (2017) 4936–4943, https://doi.org/10.1021/acs.cgd.7b00872.
[97] C. Wang, C.-R. Liu, Transcrystallization of polypropylene composites: nucleating ability of fibres, Polymer 40 (2) (1999) 289–298, https://doi.org/10.1016/S0032-3861(98)00240-7.
[98] C. Wang, F.-H. Liu, W.-H. Huang, Electrospun-fiber induced transcrystallization of isotactic polypropylene matrix, Polymer 52 (5) (2011) 1326–1336, https://doi.org/10.1016/j.polymer.2011.01.036.
[99] T. Urushihara, K. Okada, K. Watanabe, A. Toda, N. Kawamoto, M. Hikosaka, Acceleration mechanism in critical nucleation of polymers by epitaxy of nucleating agent, Polym. J. 41 (3) (2009) 228–236, https://doi.org/10.1295/polymj.PJ2008116.
[100] W. Stocker, M. Schumacher, S. Graff, A. Thierry, J.-C. Wittmann, B. Lotz, Epitaxial crystallization and AFM investigation of a frustrated polymer structure: isotactic poly(propylene), β phase, Macromolecules 31 (3) (1998) 807–814, https://doi.org/10.1021/ma971345d.

Seif Eddine Fenni earned his B.Sc. in Process Engineering in 2011 and M.Sc. in Polymer Engineering in 2013 from the University of Ferhat Abbas Setif 1 (UFAS-1) in Setif (Algeria). In 2019, he obtained a Ph.D. in Science and Technology of Chemistry and Materials under a co-tutoring program between the University of Genova (Italy) and the University of Ferhat Abbas Setif 1 (advisors: Dario Cavallo and Nacerddine Haddaoui). Subsequently (March 2019 – March 2021), he did his first post-doc experience at the University of Genova guiding several industrial-related projects. Currently, he is a Post-doctoral Fellow at Mines Paris School (PSL Research University, France). His research is focused on the crystallization, mechanical, and physical properties of multiphasic polymeric systems such as blends, biocomposites, and nanocomposites.

Alejandro J. Müller studied Materials Engineering at Simón Bolívar University, in Caracas, Venezuela. He then did an M.Sc. in Chemistry at the Venezuelan Institute for Scientific Research, IVIC, Caracas, Venezuela, and finally a Ph.D. in Physics with Andrew Keller and Jeff Odell at Bristol University, UK. He worked as a professor at the Materials Science Department of Simón Bolívar University for nearly 30 years, where he founded and led a productive research group in Polymer Science. He is a Corresponding Member of the National Academy of Engineering and Habitat from Venezuela and of the Latin-American Academy of Sciences. He won, amongst others, the Lorenzo Mendoza Fleury Prize for basic science in Chemistry given by the Polar Foundation (Caracas, Venezuela), and in 2011 he received the international "Paul J. Flory Polymer Research Prize" for his contributions to the research of Confined Crystallization. Since September 2013, he became an IKERBASQUE (Basque Science Foundation) Research Professor at POLYMAT and at the Department of Polymers and Advanced Materials: Physics, Chemistry and Technology, Faculty of Chemistry, University of the Basque Country UPV/EHU in Donostia-San Sebastián, Spain, where he leads the Polymer Physics and Advanced Manufacturing Group. He is an Editor for POLYMER (Elsevier) in the joint areas of Polymer Physics and Physical Chemistry. His fields of interest include structure, morphology, nucleation, crystallization, crystallization kinetics, rheology, and properties of multiphasic and confined polymeric materials (in particular, block copolymers, random copolymers, nano-composites, hybrids, and polymer blends).

Dario Cavallo graduated in Industrial Chemistry at the University of Genova in 2007. Afterwards he achieved the Ph.D. title in Chemical Sciences from the same University in 2011, studying polymer crystallization in “processing-relevant” conditions (supervisor: Prof. G.C. Alfonso). After the achievement of the Ph.D., he spent five months as a visiting researcher in Madrid (Spain) at the Institute of Polymer Science and Technology (ICTP-CSIC), applying infrared spectroscopy to polymorphic polymers. Subsequently (2011-2013), he was employed in a post-doc position at the Eindhoven University of Technology (The Netherlands), conducting research on structure-properties relationship in semicrystalline polymers for the Dutch Polymer Institute. Since July 2013 he became Assistant Professor at the Department of Chemistry and Industrial Chemistry of the University of Genoa and in July 2021 he was promoted to Associate Professor. His main research interests are related to the kinetics of polymer crystallization. In this framework, he focuses on various aspects of primary nucleation (including memory effects and heterogeneous nucleation at various surfaces), polymorphism, crystallization of copolymers and immiscible blends and structuring under processing conditions. The results of his research have been reported in about 114 scientific publications. He is Academic Editor for the journal “Polymer Crystallization”, furthermore he is member of the Editorial Board of the journal “Polymers” and of the International Advisory Board of “Chinese Journal of Polymer Science”.